Published in final edited form as:
Physiol Genomics. 2007 August 20; 30(3): 282–299. doi:10.1152/physiolgenomics.00242.2006.

Microarray analysis of the temporal response of skeletal muscle to methylprednisolone: comparative analysis of two dosing regimens

Richard R. Almon[1,2], **Debra C. DuBois**[1,2], **Zhenling Yao**[1], **Eric P. Hoffman**[3], **Svetlana Ghimbovschi**[3], and **William J. Jusko**[1]

[1]Department of Pharmaceutical Sciences and State University of New York (SUNY) at Buffalo, Buffalo, New York

[2]Department of Biological Sciences, State University of New York (SUNY) at Buffalo, Buffalo, New York

[3]Children's National Medical Center, Washington, District of Columbia

Abstract

The transcriptional response of skeletal muscle to chronic corticosteroid exposure was examined over 168 h and compared with the response profiles observed following a single dose of corticosteroid. Male adrenalectomized Wistar rats were given a constant-rate infusion of 0.3 $mg \bullet kg^{-1} \bullet h^{-1}$ methylprednisolone for up to 7 days via subcutaneously implanted minipumps. Four control and forty drug-treated animals were killed at ten different time points during infusion. Liver total RNAs were hybridized to 44 individual Affymetrix REA230A gene chips. Previously, we described a filtration approach for identifying genes of interest in microarray data sets developed from tissues of rats treated with methylprednisolone (MPL) following acute dosing. Here, a similar approach involving a series of three filters was applied sequentially to identify genes of interest. These filters were designed to eliminate probe sets that were not expressed in the tissue, not regulated by the drug, or did not meet defined quality control standards. Filtering eliminated 86% of probe sets, leaving a remainder of 2,316 for further consideration. In a previous study, 653 probe sets were identified as MPL regulated following administration of a single (acute) dose of the drug. Comparison of the two data sets yielded 196 genes identified as regulated by MPL in both dosing regimens. Because of receptor downregulation, it was predicted that genes regulated by receptor-glucocorticoid response element interactions would exhibit tolerance in chronic profiles. However, many genes did not exhibit steroid tolerance, indicating that present perspectives on the mechanism of glucocorticoid action cannot entirely explain all temporal profiles.

Keywords

glucocorticoids; corticosteroids; Affymetrix gene chips; gene expression; time series

Address for reprint requests and other correspondence: R. Almon, Dept. of Biological Sciences, 107 Hochstetter Hall, SUNY at Buffalo, Buffalo, NY 14260 (almon@eng.buffalo.edu)..

Glucocorticoids are a class of steroid hormones that play a central role in regulating the production, storage, use, and distribution of substrates for systemic energy metabolism. Most tissues are targets for glucocorticoid action and contribute in some way to their wide-ranging physiological effects. Synthetic glucocorticoids (corticosteroids) are used therapeutically for a wide variety of conditions that require immune and/or inflammatory modulation, including the treatment of muscular dystrophy. Because corticosteroids pharmacologically magnify the physiological actions of glucocorticoids, therapeutic use of this class of drugs is accompanied by a wide range of adverse effects including muscle wasting, hyperglycemia, dyslipidemia, hypertension, nephropathy, fatty liver, and an increased risk of arteriosclerosis (12, 20, 30, 37, 45). The musculature contributes significantly to several of these adverse effects. Corticosteroids shift the musculature into a net negative nitrogen balance, causing muscle wasting. The resultant amino acid carbon is released into circulation primarily in the form of glutamine and is taken up by the liver and kidney for use as a substrate for gluconeogenesis. The glucose is released into circulation, causing secretion of insulin. However, because corticosteroids cause insulin resistance and skeletal muscle is responsible for ~80% of the insulin-directed glucose disposal, the result is hyperglycemia (10). In addition, increased resistance in the muscle vasculature caused by corticosteroids contributes to hypertension (28).

The physiological and pharmacological effects of these compounds are complex and involve changes in the expression of many genes in multiple tissues. However, changes in expression of a single gene may involve primary and/or higher-order levels of control. A primary response can be considered as the direct transcriptional modulation of that gene by a steroid-bound receptor. Higher-order regulation may involve alteration of a secondary biosignal (which may include alteration of the expression or action of other transcription factors, either directly or indirectly, that modulate expression of that gene). Understanding the complexity of gene expression changes is a necessary first step to a comprehensive understanding of how such changes translate into altered systemic physiology and contribute to the adverse effects of corticosteroids. Within a single tissue, it is necessary to identify those genes that are regulated by steroid treatment as well as the temporal patterns of those changes following treatment.

Microarrays can provide a method for the high-throughput data collection that is necessary for constructing a comprehensive view of the transcriptional basis of such complex systemic polygenic phenomena. When microarrays are used in a rich in vivo time series, they yield temporal patterns of changes in gene expression that illustrate the cascade of molecular events in time that cause broad, complex responses. However, the magnitude of data produced in such studies provides challenges of data mining and analysis.

Previously, we described the mining and analysis of microarray time series, illustrating the responses of skeletal muscle, liver, and kidney taken from the same set of animals to a single bolus dose of the corticosteroid methylprednisolone (MPL) (4, 6, 7). Those studies included individual chips from multiple control animals as well as multiple animals at each of 16 times over a 72-h period following acute dosing with MPL. Because those experiments were initiated using adrenalecto mized animals, the drug in effect acted as a stimulus that

perturbed the homeostatic balance of the system, and the experiment monitored the deviation of the system and its return to the original state.

Although very useful, a single-dose time series only provides a limited view of the dynamics of the system in response to the drug. A pharmacological time series is different from most time series studies (for example, those assessing developmental changes) in that it can be repeated using different dosing regimens. Additional dosing regimens are valuable in that they can illustrate response profiles of genes to different patterns of input perturbations. Two genes may respond with the same temporal profile to a single-dosing regimen, suggesting that their mechanism of regulation is the same. However, they may not respond to a second dosing regimen with the same response profile, demonstrating that their mechanisms of regulation are in fact different. The results from multiple dosing regimens can therefore be used to group genes into clusters with common mechanisms of regulation. The predicating assumption is that if two or more genes have a common mechanism of regulation, then their response profiles should be the same regardless of the dosing regimen.

In the present report, we describe the use of microarrays to broadly characterize the response of skeletal muscle to both single-dose and chronic infusion of MPL. In the latter, the drug essentially serves as an unbalancing stimulus, and the experiment evaluated the capacity of the system to rebalance in the continuous presence of the drug. This data set was mined using a similar filtration approach as was applied to the acute-dosing data set, and results from both data sets were compared. Probe sets common to both filtrations were identified, allowing the coincidental evaluation of the two profiles for each gene. Examination of acute and chronic profiles clearly illustrates that corticosteroids influence the expression of genes through a wide variety of mechanisms ranging from the relatively simple, in which the chronic profile shows tolerance because of the downregulation of the glucocorticoid receptor, to very complex patterns that not only do not show tolerance but also show patterns suggesting an interplay of multiple mechanistic influences.

MATERIALS AND METHODS

Animals

Adrenalectomized male Wistar rats with body weights of 339 − 28 (SD) g were used in the study. All animals were housed in our University Laboratory Animal Facility and maintained under constant temperature (22°C) and humidity with a controlled 12:12-h light-dark cycle. A time period of at least 2 wk was allowed before animals were prepared for surgery. Rats had free access to rat chow and 0.9% NaCl drinking water. This research adheres to Principles of Laboratory Animal Care (National Institutes of Health publication no. 85-23, revised 1985) and was approved by the Institutional Animal Care and Use Committee of SUNY at Buffalo.

Forty rats were given infusions (0.3 $mg \bullet kg^{-1} \bullet h^{-1}$) of methylprednisolone sodium succinate (Solu-Medrol; The Upjohn, Kalamazoo, MI) reconstituted in supplied diluent. The infusions were administered via Alzet osmotic pumps (model no. 2001, flow rate 1 μl/h; Alza, Palo Alto, CA). The pump drug solutions were prepared for each rat based on its predose body weight. On the day of implantation, rats were anesthetized using 60–80 mg/kg ketamine and

8–10 mg/kg xylazine (im). Pumps were subcutaneously implanted between the shoulder blades on the back. Rats were killed at various times, up to 7 days. The time points included were 6, 10, 13, 18, 24, 36, 48, 72, 96, and 168 h after pump implantation. A vehicle-treated control group of four animals was implanted with a saline-filled pump and killed at various times throughout the 7-day study period (6, 18, 48, and 96 h after pump implantation). Because of the fact that pump implantation requires some time to perform, an actual *time zero* control is not possible to obtain. Therefore, the earliest experimental time point (6 h) served as the first control death time, and all controls are considered as nominal *time zero*. A more detailed description of the experiment can be found in previous reports (35, 36).

RNA preparation

Gastrocnemius muscles from each animal were ground into a fine powder in a mortar cooled by liquid nitrogen, and 100 mg of powder were added to 1 ml of prechilled Trizol Reagent (Invitrogen, Carlsbad, CA). Total RNA extractions were carried out according to the manufacturer's directions and were further purified by passage through RNeasy minicolumns (Qiagen, Valencia, CA) according to the manufacturer's protocols for RNA cleanup. Final RNA preparations were resuspended in RNase-free water and stored at −80°C. The RNAs were quantified spectrophotometrically, and purity and integrity were assessed by agarose gel electrophoresis. All samples exhibited 260/280 absorbance ratios of ~2.0, and all showed intact ribosomal 28S and 18S RNA bands in an approximate ratio of 2:1 as visualized by ethidium bromide staining.

Kinetic-based quantitative RT-PCR

Kinetic-based RT-PCR assessment of myostatin mRNA was carried out using TaqMan-based fluorescent probes in a MX3000 fluorescence-based thermocycler (Stratagene, La Jolla, CA). A one-tube/two-enzyme assay design employing the Brilliant 1-Step Quantitative Core Reagent Kit (Stratagene) was used according to the manufacturer's directions. Concentrations of $MgCl_2$ were 3 mM, forward and reverse probe concentrations were 200 nM, and probe concentrations were 100 nM. Probe and primers were designed using PrimerExpress software (Applied Bio-systems, Foster City, CA), and the sequences used shared no homology with other known rat sequences. Probe and primers were custom synthesized by Biosearch Technologies (Novato, CA) and contained a FAM label on the 5’-end and black hole quencher (BHQ1) on the 3’-end. The sequences were as follows: forward primer, 5’-TTGGATGAGAATGGGCATGA-3’; reverse primer, 5’-ACCTCTTGGGTGTGTCTGTTACT-3’; and probe, 5’-CTTGCTGTAACCTTCCCAGGACCAGGA-3’. Amplicon length was 103 bp. Signals were quantified against cRNA standards prepared from the myostatin coding sequence cloned into pCR II TOPO vector (Invitrogen) and were prepared by in vitro transcription using T7 Megascript Kits (Ambion, Austin, TX). Samples were normalized to the amount of total RNA in each assay tube. Seven cRNA standards were run concurrently on the same plate in duplicate with tissue RNA samples, which were run in triplicate. RT minus controls were also run on the same plate for each sample to test for possible genomic contamination of RNA samples and in all cases gave no measurable amplification signal. Intra- and interassay coefficients of variation were <18%.

Microarrays

Isolated RNA from each muscle sample was used to prepare the target according to the manufacturer's protocols. The biotinylated cRNAs were hybridized to 44 individual Affymetrix GeneChips, Rat Genome 230A (Affymetrix, Santa Clara, CA), that contained 15,967 probe sets. These gene chips contain over 7,000 more probe sets than the ones used (U-34A) in our previous acute-dose MPL study in muscle (6). The high reproducibility of in situ synthesis of oligonucleotide chips allows accurate comparison of signals generated by samples hybridized to separate arrays.

Data analysis and public access

All data reported here are available to the public via both the Public Expression Profiling Resource (PEPR) and the National Center for Biotechnology Information (NCBI) Gene Expression Omnibus (GEO), as raw and processed (probe set algorithm) data. In PEPR (http://pepr.cnmcresearch.org), all data are preprocessed into five probe set algorithms [DNA Chip Analyzer (dCHIP) perfect match, dCHIP mismatch model, robust multichip average (RMA), Microarray Suite (MAS)5.0, and ProbeProfiler] and available for dynamic queries. For this present manuscript, we opted to use MAS5.0 probe set algorithms. While other probe set algorithms have been shown to show better performance than MAS5.0 (23, 46), we have made both raw data and five probe set interpretations available to the public. For Affymetrix MAS5.0, signal intensities were normalized for each chip using a distribution of all genes around the 50th percentile. The data set was then loaded into a data mining program, GeneSpring 7.0 (Silicon Genetics, Redwood City, CA). The generated data set has been submitted to the NCBI GEO database (http://www.ncbi.nlm.nih.gov/ projects/ geo/; accession no. GSE5101).

The first step in the analysis involved screening the data from the 11 groups of 4 animals for variance anomalies. This was an important consideration, since the four control animals used in this study were killed at various times (6, 18, 48, and 96 h) within the experimental time frame. This step involved calculation of the mean, standard deviation, and coefficient of variation (CV) of the raw data for each of the 15,967 individual probe sets on the four chips at each individual time point (data from 4 drug-treated animals killed at the same time point) and for the controls (data from 4 vehicle-treated animals killed at 4 different time points). The range of the CVs for each gene at each time point was 40.8–50.2%. The average CV for the drug-treated samples was 44.8%, and the CV for the control group was 44.6%.

Before screening for probe sets with altered expression levels, the data set was normalized again to the mean values of control samples so that all probe sets from control samples had a mean value of 1, and probe sets from treated animals had a value of either greater than, less than, or equal to 1, representing upregulation, downregulation, or no change, respectively. At present, there are a variety of probe set algorithms available to apply to gene array data sets. Most of these are designed to select probe sets that discriminate one group from another. All of these algorithms, MAS5.0, RMA, GC-RMA, and Probe Logarithmic Intensity Error (PLIER), have strengths and weaknesses, and none is designed to take advantage of the unique strengths afforded by a rich time series (38). For our initial analysis

of this data set, our objective was to select with a very high certainty those probe sets that were regulated by corticosteroids. To accomplish this goal, the normalized probe sets were then filtered with a series of predetermined screening criteria to identify probe sets with appreciable expression levels, expression changes, and acceptable data quality. This set of filters is approximately the same as was used to analyze the acute-dosing data sets with minor modifications to accommodate the different number of samples/chips in the two experiments (4, 6, 7).

The process of data mining was performed in the GeneSpring program, and the progress after each step was visualized using the gene tree cluster feature of the program. This cluster feature rearranges the order of the probe sets and groups them based on the similarity (Pearson's correlation) of their expression dynamics. Then the probe sets that were not eliminated by the filter were displayed vertically as a gene tree, and their expression dynamics over time were displayed horizontally in colors. Yellow in the graph represents an expression ratio around 1, or no change. The color progressing toward red indicates a normalized value >1, or upregulation, and the color toward blue indicates a value <1, or downregulation from control levels. The brightness of the colors reflects the original signal intensities or expression levels before normalization. The more abundantly expressed mRNA exhibit the brighter color. Figure 1 shows the gene tree of the entire data set (15,967 probe sets). The *x*-axis represents the 11 time points including vehicle controls (nominally *time 0*). The *y*-axis represents the list of the probe sets in the order of similarity. Figure 2, *top*, shows a magnification of four probe sets with an apparent response of enhanced expression taken from the tree shown in Fig. 1. A significant deficit of the gene tree representation is that all time intervals are represented as equal, and therefore to some degree temporal patterns are misrepresented. This is illustrated in Fig. 2, *bottom*, which shows a linear plot of the data for the four probe sets presented at Fig. 2, *top*. This plot also illustrates the relationship between intensity of color and signal. The lightest probe set in the gene tree is the *bottom* plot, while the most intensely colored probe set is the *top* plot. Similarly, Fig. 3 shows a magnification of five probe sets with apparent downregulation as well as linear plots of these five probe sets. As illustrated in these two examples, it is possible to visually identify genes under regulation using gene trees. However, this approach does not entail objective criteria for selection of probes for further consideration.

To screen for regulated probe sets objectively, the entire data set was filtered with criteria similar to the ones applied to the data set from an acute-dose MPL experiment (4, 6, 7). This approach does not select for probe sets but rather eliminates those probe sets that do not meet certain criteria, leaving the remainder for further consideration. The first filter was designed to eliminate probe sets for genes that are not expressed in the muscle. This filter enlisted a function in Affymetrix MAS5.0. During initial data analysis, a “call” of present (P), absent (A), or marginal (M) for each probe set on each chip was generated based on the intensity comparison of the matched and mismatched probe sequence pairs. The PM/MM comparison was designed to be used for comparisons at terminal points in time of binary nature (benign vs. malignant, type A vs. type B, etc.) and is the subject of much discussion when considering probe set algorithms (38). We employed the PM/MM comparison in a limited manner as a filter. The first filter is based on the logic that, if the gene is expressed in

the tissue, then PM should be greater than MM at least on a small percentage of the chips. Therefore, the first filter eliminated all probe sets that did not have a call of P on at least 3 of the 44 chips (3P). This filter eliminated 6,151 probe sets, leaving a remainder of 9,816 for further consideration. Those probe sets that were not eliminated are presented as a gene tree in Fig. 4. These genes are more likely to be expressed in rat muscle than those that were eliminated.

The second level of filtering was designed to eliminate probe sets that could not meet the basic criterion of a regulated probe. Specifically, this filtering approach eliminates probe sets whose average did not deviate from baseline by a certain value for a reasonable number of time points and employed two filters that were designed to eliminate probe sets that were neither down- nor upregulated. The first of these filters eliminated probe sets that could not meet a minimal criterion for downregulation. Starting with the 3P filtered list, we eliminated all probe sets that did not have average values <0.65 in at least two conditions (time points). Those that were not eliminated by this filter were retained as potentially downregulated probe sets. The next filter was designed to eliminate probe sets that could not meet a minimal criterion for upregulation. Starting with the 3P filtered list, we eliminated all probe sets that did not have average values >1.5 in at least two conditions (time points). Those that were not eliminated by this filter were retained as potentially upregulated probe sets. However, there were a small number of probe sets that were not eliminated by either filter. Using a Venn diagram, we removed these from both lists and created a list of probe sets with potential complex regulation. Figure 5 shows gene trees of the potential downregulated probe sets (1,466), upregulated probe sets (1,412), and a group of probe sets (60) that met both criteria.

The last filter addressed the quality of the data. For this “quality control” filter, we eliminated probe sets that did not meet two conditions. The first condition focused on the control chips. As indicated above, our initial operation was to divide the value of each individual probe set on each chip by the mean of the values for that probe set on the four control chips. Therefore, the quality of the control data for each probe set is of particular importance in defining regulation by the drug. This filter eliminated probe sets whose control values exhibited CVs >50%. The CV% of the entire data set was 44.8%, and that of the controls was 44.6%. The 50% cutoff was chosen to approximate the quality of the entire data set. The second condition focused on the remaining 10 time points. This filter also eliminated probe sets whose CV for more than 5 of the remaining 10 time points exceeded 50%. Following the application of this filter, 2,316 probe sets remained for consideration. Of the 2,316, 1,226 were in the upregulated list, 1,065 were in the downregulated list, and 25 were in the list that met both criteria. Figure 6 shows a gene tree of all 2,316 remaining probe sets. The three lists are provided as Supplemental Material (supplemental data are available at the online version of this article).

RESULTS

Figure 7, *top*, presents concentrations of MPL in plasma of animals receiving chronic MPL administration through Alzet pumps. By 6 h, MPL concentrations reach a stable steady state that is maintained throughout the 7-day infusion period. In contrast, single MPL doses (Fig.

7, *bottom*) result in drug concentrations that dissipate in a biexponential fashion and fall below the level of detection by 7 h. Analyses of MPL kinetics for both acute (40, 42) and chronic (35, 36) dosing have been described previously.

Data mining of gene arrays from the chronic MPL treatment series identified 2,316 MPL-regulated probe sets on the R230A gene chips. Muscle samples from animals previously given single-dose MPL were collected in a time series that involved 16 time points over a 72-h period. RNAs from those muscles were applied to the older Affymetrix RU34A chip. A similar filtering scheme applied to that data set identified 653 probe sets as being regulated by MPL. Using Affymetrix homology tables and basic local alignment search tool (Blast) searches, we identified 241 probe sets of the 653 on the U34A chip that corresponded to 219 of the 2,316 identified probe sets on the U230A chip. Because both chips in some cases contain multiple probe sets for the same gene, and because there is a higher degree of probe set redundancy on the older U34A chip, the numbers of corresponding probe sets common to the two chips are not equal. Likewise, the number of genes actually represented in this common set is less than the number of probe sets.

We identified 196 genes that were regulated by MPL in response to both dosing regimens. Most likely, this list does not contain all genes regulated by MPL in skeletal muscle. A perusal of both data sets indicates that there were many probe sets that failed the quality control filter on one of the two chips and were thus eliminated. Nonetheless, these 196 genes have a very high degree of certainty of being regulated by MPL in the muscle. In addition, the two profiles taken together provide an important foundation for understanding the mechanisms underlying the drug's regulation of genes in the skeletal muscle.

Diversity of response profiles

When the individual probe set profiles from acute and chronic dosing are viewed together, it is clear that multiple patterns of changes in mRNA expression occur. For example, Figs. 8–10 show representative examples of diverse response profiles of enhanced mRNA expression. Figure 8 shows acute and chronic expression profiles of two genes, mitogen-activated protein kinase-14 (MapK14) and peroxisome proliferator-activated receptor-δ (PPARδ), where there is a transient enhanced expression with return to baseline following both treatments. These profiles are very similar to the expression of tyrosine aminotransferase (TAT) in liver, a well-established marker for the enhancement of gene expression by glucocorticoids. We have previously characterized TAT mRNA expression by Northern hybridization in livers taken from the same animals used in these acute and chronic studies (35, 40). Like TAT, both MapK14 and PPARδ exhibit tolerance in that these genes almost recover to their baseline after a period of time despite the continuous presence of the drug (35). Tolerance is not unexpected in light of the well-documented phenomena of glucocorticoid-induced downregulation of its own receptor. It should be noted that in earlier reports, we showed that the glucocorticoid receptor (GR) is strongly downregulated in response to MPL in both muscle and livers from these same animals (34–36, 40, 41). Since GR mediates the effect of the drug, the large reduction in this effector molecule should greatly reduce the driving force for changes in gene expression. Therefore, for genes exhibiting enhanced expression mediated by GR binding to glucocorticoid response

elements (GREs; primary regulation), it is expected that both acute and chronic dosing would produce an initial enhanced expression followed by a return to baseline despite the continuous presence of the drug.

However, not all profiles exhibiting enhanced expression show tolerance. For example, Fig. 9 shows the response profiles of two genes, glutamine synthetase (GS) and eukaryotic translation initiation factor-4E binding protein-1 (Eif4ebp1), following both acute and chronic treatment. In both cases, the acute profile is very similar to those of the genes discussed above, with a transient increase followed by a return to baseline. It should be noted that we have previously reported this same profile for GS expression in muscles following acute dosing, as measured by Northern hybridization (34). However, the response profile of both genes presented in Fig. 9 to chronic infusion is entirely different, in that enhanced expression remains for at least 96 h.

The response profiles shown in Figs. 8 and 9 do not encompass the entire repertoire of acute and chronic response profiles. For example, Fig. 10 shows the response profiles of interleukin-6 receptor (IL6R1) and interferon-related developmental regulator-1 (Ifrd1). Again, with acute treatment, there is a sharp peak of enhanced expression followed by a return toward baseline. With chronic treatment, there is an initial enhanced expression that appears to initially decrease toward baseline, but this is followed by a second higher level of enhanced expression. These genes appear as if they are going to return toward baseline, but at some time after 24 h of infusion some additional enhancing influence seems to intervene.

Thus, when the response profiles to two different dosing regimens are viewed together, it is very clear that a single profile by itself is not adequate to group genes into clusters with common mechanisms of regulation. A diversity of response profiles also exists for genes whose expression is downregulated by MPL. Figure 11 shows the response profiles of Syndecan 2, core protein (Sdc2). Both the acute and chronic profiles show a transient downregulation and a return toward baseline but an inability to fully recapture the baseline. In contrast, both the chronic and acute profiles of Na-K-Cl co-transporter (Nkcc1), presented in Fig. 12, show a transient downregulation followed by a period of enhanced expression with an eventual return toward baseline. Another variation in the chronic expression profile of genes that show downregulation are those with little or no recovery, as can be seen in Fig. 13. Both myristoylated alanine-rich C-kinase substrate (Macs) and extracellular signal-related kinase-3 (ERK3) show a transient downregulation in the acute profile. However, in the chronic profile, Macs shows almost no recovery of baseline throughout the infusion period, while ERK3 shows a very slow progression back toward baseline.

Some genes exhibited more complex patterns involving both enhanced and repressed regulation. As illustrated by myogenic factor-6 (Myf6), presented in Fig. 14, the acute profile showed an initial downregulation in the first 4 h after dosing followed by a secondary upregulation. The chronic profile exhibited only the secondary enhanced regulation. Most likely, the chronic profile was unable to capture the initial downregulation because the first time point was taken after 6 h of infusion. By necessity, this was the first time point in this study because steady-state plasma MPL was only obtained at 6 h after pump implantation.

Together, the data presented in Figs. 8–14 illustrate that changes in gene expression in response to corticosteroids clearly involve multiple mechanisms.

Gene groupings and expression profiles

Of the total of 196 genes, 33% were downregulated, 43% were upregulated, and the remaining 24% were classified as complex following one or both dosing regimens. We conducted a literature search for all 196 genes primarily using the NCBI “search across databases” feature. On the basis of this information and domain knowledge, we grouped the 196 genes based primarily on function with two additional groups based on subcellular localization (mitochondrial and plasma membrane). These groups are presented in Tables 1–8 and list identifying criteria as well as temporal responses following both acute and chronic treatments. For each gene on the tables, we provide the probe set identification number for the gene on the 230A chip (chronic) and the U34A chip (acute). We also characterize the response of the gene to both dosing regimens as upregulated (up), downregulated (down), or complex (some combination of both). Although not perfect, these groupings together with the expression profiles provide insight into the global impact of corticosteroids on the skeletal muscle.

The most highly populated group is termed “transcription-translation” and contains 47 genes (Table 1). The majority of genes in this group are transcription factors, indicating that a major influence of corticosteroids is derived from their ability to alter the effect of other influences on transcription. Alteration in expression of a transcription factor would likely serve as a secondary biosignal altering the expression of other genes. Since alterations in the amount of messages only have an impact once they are reflected as changes in protein, the consequence of these changes should be delayed in time. Such a time delay may therefore explain at least some of the genes that express complex higher-order regulation. Of particular interest in this group, because of their relationship to the control of muscle gene expression (11), is the downregulation in both response profiles of myogenin and myogenic factor D (MyoD), as well as the more complex response of myogenic factor-6 (Fig. 14), which shows upregulation in the acute profile and transient downregulation followed by sustained upregulation in the chronic profile.

A second highly populated group is termed “signaling,” with 37 members (Table 2). Thirteen genes in this group show upregulation in both the acute and chronic profiles and 15 show downregulation in both acute and chronic profiles. As might be expected, this group is dominated by kinases and phosphatases. We have also included in this group several membrane receptors that could have been included in the “membrane” group but were included in this group because of their involvement in signaling. As with transcription factors, alterations in the expression of signaling proteins may act as secondary biosignals that modulate the expression of other genes. Obviously missing in this group is myostatin, which is important to the maintenance of muscle mass (22, 24). Although this gene was retained in the filtering of the acute data set, it was eliminated by the quality control filter in the chronic data set because the CV of the controls was 80%. Because of the potential importance of this gene to muscle atrophy, Fig. 15 provides the gene array data of acute and chronic profiles for myostatin. Also presented in Fig. 15 is myostatin message measured by

quantitative RT-PCR after chronic treatment, confirming the profile obtained by arrays. In both chronic and acute profiles, there is a strong upregulation followed by a rather shallow but sustained downregulation.

The group termed “plasma membrane” contains 23 genes (Table 3). Because the surface membrane of a cell mediates its interaction with the external environment, this group by necessity is difficult to distinguish from the signaling group. The “immune-related” group contains 18 genes (Table 4). Some of these genes, such as interleukin-6 receptor and the interferon-γ receptor, could be included in the signaling or plasma membrane groups. However, because the pharmacological use of corticosteroids is to modulate immune/inflammatory processes, we chose to list these separately. The next most populated group is best characterized as “vascular” and contains 16 genes (Table 5). This group contains genes such as angiotensin-converting enzyme, which influences vascular tone (31), as well as genes such as vascular endothelial growth factor, which influences angiogenesis (27). The next group contains 12 genes related to “protein and amino acid metabolism” (Table 6). Two genes in this list are of particular interest because of their potential involvement in the muscle atrophy caused by corticosteroids: GS and ring finger protein-28 (MURF1) (13). As can be seen in Fig. 9, following the acute dose, there is a rather rapid rise in GS expression followed by a relatively slow decline. However, the chronic profile is rather unusual in that the mRNA remains elevated for an extended period of time and only declines after 96 h. Figure 16 shows the profiles for MURF1. Although the acute profiles for GS and MURF1 are quite similar, the chronic profiles are somewhat different. Following chronic infusion, MURF1 reaches an early peak, remains high for 48 h, and then declines quite slowly over the remainder of the 168-h infusion period. The next group of genes, containing 10 members, is termed “nuclear-encoded mitochondrial genes” (Table 7). The dominant trend in these genes is a decrease which may reflect the almost 30% loss in mass of the gastrocnemius muscle (36). Table 8 contains the remaining 34 genes and is classified as “other.” Table 8 contains genes involved in various processes. For example, glutathione peroxidase-3 and microsomal glutathione *S*-transferase-2 are associated with oxidative stress. Table 8 also contains several genes involved in small molecule metabolism, such as sulfotransferase-1a1, cytochrome *P*-450 4b1, cytosolic cysteine dioxygenase-1, flavin-containing monooxygenase-1, and *S*-adenosylmethionine decarboxylase-1, all of which are upregulated on both profiles (19). Finally, Table 8 contains four expressed sequence tags that could not be identified by Blast searches.

DISCUSSION

This report describes the mining of a microarray data set obtained from the analysis of skeletal muscles from a population of adrenalectomized animals given a chronic infusion of MPL for up to 1 wk. Muscle RNA from 4 control animals and 4 animals killed at each of 10 time points over a 168-h period was applied to individual Affymetrix R230A chips. The data set was mined using a filtering approach similar to the one applied to data sets developed from skeletal muscles, livers, and kidneys of animals treated with a single bolus dose of MPL, where animals were killed at 16 time points following dosing and compared with untreated controls (4, 6, 7). This filtration approach does not select for probes but rather

eliminates probe sets that do not meet explicit requirements. Those probe sets not eliminated are retained for analysis.

The filtration yielded a remainder of 2,316 probe sets for further consideration. These probe sets were compared with 653 probe sets that remained following filtering of the data set obtained following the single dose of MPL (6). This comparison yielded 241 probe sets in the acute-dosing data set that corresponded to 219 probe sets in the chronic infusion data set. The results identified 196 different genes regulated by both dosing regimens. Because the filtering process is quite stringent, these 196 genes most likely do not include all genes regulated by MPL in the tissue. However, they do provide a basis for evaluating the global effects of corticosteroids on skeletal muscle. It is probable that, had we employed one of the other presently available probe set algorithms, we would have obtained a broader selection of probe sets. All of these algorithms have strengths and weaknesses, with none being optimal for all purposes, especially time series data. For example, GC-RMA shows good performance in organisms with few confounding variables (e.g., yeast) but results in many false positives in rats (38). Our initial analysis was quite stringent and employed no single algorithm. However, given the public availability of our data sets and the active evolution of algorithms for mining and clustering gene array time series data sets, we expect that these data sets will be revisited in the future as new tools become available. Of particular potential for these two data sets is the evolution of algorithms for biclustering (15).

The objective of obtaining two time series profiles for each gene is to identify genes with common mechanisms of regulation. The hypothesis is that if two or more genes have common mechanisms of regulation, then they should have the same temporal profile in response to all dosing regimens. There are available a variety of clustering methods designed to group genes based on their profiles (8, 9). However, at present, no analytic method is available to cluster using two time series profiles, viz., “biclustering.” Our filtering approach crudely identifies genes that meet minimal criteria for “up-” and “down”-regulation based on deviation from baseline. In both the acute and chronic data sets, some profiles met both criteria, suggesting complex regulation. We visually inspected all profiles (241 acute and 219 chronic) and categorized each based on up- or down-deviation from baseline. In many cases, because of probe set redundancy, more than one profile was available for acute, chronic, or both. These instances are noted on the tables. With this information, we proceeded to evaluate acute and chronic profiles together. Solely on the basis of this crude classification, we identified three basic patterns. For >75% of the genes, the profile was either up or down in both the acute and chronic profiles. In the remaining cases, the profiles were complex, involving both up- and downregulation. However, closer analysis, as presented in Figs. 8–16, illustrates that, even with the consideration of the <75% of the genes where the profiles were either both up or both down, there still remains considerable diversity in mRNA expression patterns and therefore presumably in mechanisms of regulation.

The generally accepted mechanism for most glucocorticoid effects involves binding of free steroid to a cytoplasmically localized receptor, translocation of ligand-bound receptor to the nucleus, binding of a ligand receptor dimer to a specific DNA site (GRE), and modulation of the amount of selective mRNAs (42). Although some effects on mRNA stability have been

noted, a common mechanism involves increasing or decreasing the rate of transcription of particular genes. In studies of the enzyme TAT in liver involving both a repeated dosing and a chronic-dosing paradigm, we described the phenomena of steroid tolerance (35, 36, 41). In those and other reports, we demonstrated that MPL treatment caused a rather long-lived downregulation of the glucocorticoid receptor (mRNA and protein) in both skeletal muscle and liver. In addition, when a second dose was administered before full recovery of receptor, the enhanced expression of TAT (mRNA and protein) was reduced in proportion to the reduced concentration of receptor (41). In subsequent studies, we found that chronic infusion of MPL caused a sustained downregulation of the receptor (mRNA and protein) and that the expression of TAT (mRNA and protein) returned back toward the baseline in the continuous presence of the drug (35, 36). If the glucocorticoid receptor alone mediates the effect of the drug, then this is a rational result. Figures 8 and 15 show that the acute and chronic profiles of MAPK14, PPARδ, and myostatin come close to approximating a chronic profile of tolerance. Similarly, Fig. 11 to some degree approximates this result for downregulation. However, throughout the course of MPL infusion, the muscles continuously atrophied (36). Thus the response of the muscles to the continuous infusion suggests that those genes involved in effecting the atrophy should not show tolerance. It has been suggested that upregulation of myostatin may be involved in chronic muscle atrophy . However, the fact that myostatin only shows a transient upregulation followed by downregulation suggests that myostatin may not be involved in chronic atrophy caused by infusion of MPL. In contrast, the more sustained upregulation of GS, MURF1, and Eif4eBP supports their involvement in chronic atrophy. Similarly, the sustained downregulation of Macs and ERK3 supports their involvement in the chronic and continuous effects of corticosteroids on skeletal muscle, such as insulin resistance and atrophy (5).

However, the major question posed by a perusal of the profiles that do not show tolerance is as follows. How can the drug continue to have sustained strong effects when the receptor is greatly diminished to the point of almost being gone? One rational possibility is that our concept of the structure and function of the GRE is entirely too simplistic. If multiple GREs with greatly different affinities for the drug receptor complex exist, then the type of result seen for genes that show more sustained up- or downregulation could be explained. An additional complexity might operate if different isoforms of GR, as suggested by the work of Lu and Cidlowski (32), are interacting with multiple GREs. Another possibility is that our concept of only GR mediating corticosteroid effects may be simplistic, and some other “receptor” or interactions with other transcription factors are involved. This possibility is suggested by the chronic profile for IL6R and Ifrd-1 seen in Fig. 10. Initially, it appears as if both of these genes are going to respond with patterns similar to profiles for Mapk14 and PPAR† and return to baseline, but the expression is enhanced again to even higher levels. An alternative but related possible mechanism that could result in similar patterns of expression is the regulation of a secondary biosignal by glucocorticoids that in turn further modulates the expression of a glucocorticoid-regulated gene. Obvious candidates for potential biosignals would, of course, be other known transcription factors. As illustrated in Table 1, a large number of transcription factors are themselves modulated by MPL. In any case, the results clearly demonstrate that at present, there is much we do not know about how corticosteroids influence gene expression.

We attempted to sort the 196 genes into groups based on a domain knowledge ontology. Table 1 demonstrates the broad impact these drugs have on transcription and translation. Of particular interest is the downregulation in both the acute and chronic profiles of myogenin and MyoD. These are two of four basic-helix-loop-helix transcription factors that are important for expressing muscle phenotype (11, 22). The upregulation of Id1 in both profiles is consistent with a reduced influence of these muscle regulatory factors, since Id1 has been shown to bind to and inhibit these basic-helix-loop-helix transcription factors in skeletal muscle (47). Unexpectedly, a third one of the four, Myf6, shows a transient downregulation followed by upregulation in the acute profile and a delayed upregulation in the chronic profile (Fig. 14). It should be noted that the fourth member of this group of transcription factors, Myf5, is not represented by a probe set of the Affymetrix chips. The upregulation of both PPARα and PPARδ is also quite relevant to the condition of the metabolic syndrome caused by corticosteroids. Both transcription factors are important for regulating fatty acid oxidation in skeletal muscle and may relate to corticosteroid-induced insulin resistance (5, 21, 39).

In interpreting these results, it is important to keep in mind that skeletal muscles contain satellite cells in addition to multinucleated fibers. The downregulation of Meox2, a gene that appears to be upstream of the expression of both MyoD and myogenin (33), suggests the possibility that corticosteroids are suppressing the expression of muscle phenotypes in the satellite cell population.

Although the signaling table is dominated by kinases and phosphatases, one unexpected result is the downregulation of IGFBP5 in both profiles. It has been suggested that the up-regulation of IGFBP5 may play a role in muscle atrophy by sequestering IGF-I (26). Interestingly, IGFBP3 is upregulated in both profiles. However, the fact that corticosteroids down-regulate the expression of IGF-I may make changes in expression patterns of the binding proteins much less relevant to corticosteroid-induced atrophy (44). It has also been suggested that IL6 is associated with muscle atrophy conditions (44). The sustained upregulation of the IL6 receptor in both profiles is consistent with this possibility. Similarly, the sustained upregulation of Eif4ebp1 is consistent with corticosteroids inhibiting protein synthesis, while the upregulation of both MURF1 and GS is consistent with increased protein degradation (13, 29, 34). Previously, we presented data supporting the hypothesis that both denervation and disuse atrophy are caused by a muscle becoming hypersensitive to circulating glucocorticoids (1–3, 16–18). In the intervening years, aspects of this hypothesis have been examined by others (24, 25, 43). With the single exception that IGFBP5 is upregulated following hindlimb suspension, whereas this gene is clearly downregulated by corticosteroids, the initial hypothesis still seems reasonable.

The use of a rich time series such as this for examining patterns of changes in gene expression can be more informative than single time point studies for several reasons. The data presented here illustrate that, to simply categorize a gene as upor downregulated is too simplistic, as multiple different patterns of up- and downregulation occur following corticosteroid treatment. Characterization of the magnitude of expression change using single time point studies can also be misleading, since the magnitude of change will be dependent on the particular time point examined. In fact, with complex biphasic regulation,

a change in expression may be categorized as up at one point in the time series but not changed or down at a different time point. For these reasons, we did not attempt to list magnitude of change in Tables 1–8.

Finally, the two data sets together illustrate the need for data mining tools that are capable of the coincidental analysis of more than one temporal profile. Our approach to filtering in many respects was too stringent. Not only was the upregulated myostatin marginally eliminated in one of the two filtered data sets, but also, other clearly relevant genes such as the downregulated insulin receptor substrate-1 (IRS-1) were eliminated by filtering in one of the two data sets. We anticipate that, as additional tools become available, these data sets will be revisited many times.

All data sets described in this and related cited publications are available online in GEO. It is our intent to make these data sets, as well as our related data sets on other tissues taken from these same animals, widely available to other researchers. For this reason, all data are also available online at the PEPR site (http://pepr.cnmcresearch.org) developed and maintained by the Children's National Medical Center, Microarray Research Center (14). These data are in a user friendly format, where individual temporal profiles are searchable and all data can be obtained and used without requirement for any additional specialized software.

Supplementary Material

Refer to Web version on PubMed Central for supplementary material.

Acknowledgments

GRANTS

This work was supported by National Institutes of Health (NIH; Bethesda, MD) Grants GM-24211 and GM-67650 and by a grant from the National Aeronautics and Space Administration. This data set was developed under the auspices of a grant from the National Heart, Lung, and Blood Institute/NIH Programs in Genomic Applications (HL-66614).

REFERENCES

1. Almon RR, DuBois DC. Adrenalectomy eliminates both fiber-type differences and starvation effects on denervated muscle. Am J Physiol Endocrinol Metab. 1988; 255:E850–E856.
2. Almon RR, DuBois DC. Are there conditions in which adrenalectomy impedes the atrophying effects of denervation? Physiologist. 1985; 28:S69–S70. [PubMed: 3834490]
3. Almon RR, DuBois DC. Fiber-type discrimination in disuse and glucocorticoid-induced atrophy. Med Sci Sports Exerc. 1990; 22:304–311. [PubMed: 2199752]
4. Almon RR, DuBois DC, Jin JY, Jusko WJ. Pharmacogenomic responses of rat liver to methylprednisolone: an approach to mining a rich microarray time series. AAPS J. 2005; 7:E156–E194. [PubMed: 16146338]
5. Almon RR, DuBois DC, Jin JY, Jusko WJ. Temporal profiling of the transcriptional basis for the development of corticosteroid-induced insulin resistance in rat muscle. J Endocrinol. 2005; 184:219–232. [PubMed: 15642798]
6. Almon RR, DuBois DC, Piel WH, Jusko WJ. The genomic response of skeletal muscle to methylprednisolone using microarrays: tailoring data mining to the structure of the pharmacogenomic time series. Pharmacogenomics. 2004; 5:525–552. [PubMed: 15212590]

7. Almon RR, Lai W, DuBois DC, Jusko WJ. Corticosteroid-regulated genes in rat kidney: mining time series array data. Am J Physiol Endocrinol Metab. 2005; 289:E870–E882. [PubMed: 15985454]
8. Androulakis, IP.; Vitolo, J.; Roth, CM. Proc Foundations Systems Biol Engineering. Santa Barbara, CA: 2005. Selecting maximally informative genes to enable temporal expression profiling analysis..
9. Arai K, Lee K, Berthiaume F, Tompkins RG, Yarmush ML. Intrahepatic amino acid and glucose metabolism in a d-galactosamine-induced rat liver failure model. Hepatology. 2001; 34:360–371. [PubMed: 11481621]
10. Bao S, Kennedy A, Wojciechowski B, Wallace P, Ganaway E, Garvey WT. Expression of mRNAs encoding uncoupling proteins in human skeletal muscle: effects of obesity and diabetes. Diabetes. 1998; 47:1935–1940. [PubMed: 9836527]
11. Bergstrom DA, Tapscott SJ. Molecular distinction between specification and differentiation in the myogenic basic helix-loop-helix transcription factor family. Mol Cell Biol. 2001; 21:2404–2412. [PubMed: 11259589]
12. Bialis M, Routledge P. Adverse effects of corticosteroids. Adverse Drug React Toxicol Rev. 1998; 17:227–235. [PubMed: 10196628]
13. Bodine SC, Latres E, Baumhueter S, Lai VK, Nunez L, Clarke BA, Poueymirou WT, Panaro FJ, Na E, Dharmarajan K, Pan ZQ, Valenzuela DM, Dechiara TM, Stitt TN, Yancopoulos GD, Glass DJ. Identification of ubiquitin ligases required for skeletal muscle atrophy. Science. 2001; 294:1704–1708. [PubMed: 11679633]
14. Chen J, Zhao P, Massaro D, Clerch L, Almon RR, DuBois DC, Jusko WJ, Hoffman E. The PEPR genechip data warehouse, and implementation of a dynamic time series query tool (sgqt) with graphical interface. Nucleic Acids Res. 2004; 32:D578–D581. [PubMed: 14681485]
15. Cheng Y, Church GM. Biclustering of expression data. Proc Int Conf Intell Syst Mol Biol. 2000; 8:93–103. [PubMed: 10977070]
16. DuBois DC, Almon RR. Disuse atrophy of skeletal muscle is associated with an increase in number of glucocorticoid receptors. Endocrinology. 1980; 107:1649–1651. [PubMed: 7428684]
17. DuBois DC, Almon RR. Glucocorticoid sites in skeletal muscle: adrenalectomy, maturation, fiber type, and sex. Am J Physiol Endocrinol Metab. 1984; 247:E118–E125.
18. DuBois DC, Almon RR. A possible role for glucocorticoids in denervation atrophy. Muscle Nerve. 1981; 4:370–373. [PubMed: 7290104]
19. Ehrhart J, Gluck M, Mieyal J, Zeevalk FD. Functional glutaredoxin (thioltransferase) activity in rat brain and liver mitochondria. Parkinsonism Rel Disord. 2002; 8:395–400.
20. Frauman A. An overview of the adverse reactions to adrenal corticosteroids. Adverse Drug React Toxicol Rev. 1996; 15:203–206. [PubMed: 9113247]
21. Guillet-Deniau I, Mieulet V, Le Lay S, Achouri Y, Carre D, Girard J, Foufelle F, Ferre P. Sterol regulatory element binding protein-1C expression and action in rat muscles: insulin-like effects on the control of glycolytic and lipogenic enzymes and UCP3 gene expression. Diabetes. 2002; 51:1722–1728. [PubMed: 12031958]
22. Guttridge DC. Signaling pathways weigh in on decisions to make or break skeletal muscle. Curr Opin Clin Nutr Metab Care. 2004; 7:443–450. [PubMed: 15192448]
23. Irizzary RA, Bolstad BM, Collin F, Cope LM, Hobbs B, Speed TP. Summaries of Affymetrix genechip probe level data. Nucleic Acids Res. 2003; 31:E15. [PubMed: 12582260]
24. Jackman RW, Kandarian SC. The molecular basis of skeletal muscle atrophy. Am J Physiol Cell Physiol. 2004; 287:C834–C843. [PubMed: 15355854]
25. Jagoe RT, Lecker SH, Gomes M, Goldberg AL. Patterns of gene expression in atrophying skeletal muscles: response to food deprivation. FASEB J. 2002; 16:1697–1712. [PubMed: 12409312]
26. Kamei Y, Miura S, Suzuki M, Kai Y, Mizukami J, Taniguchi T, Mochida K, Hata T, Matsuda J, Aburatani H, Nishino I, Ezaki O. Skeletal muscle FOXO1 (FKHR) transgenic mice have less skeletal muscle mass, down-regulated Type I (slow twitch/red muscle) fiber genes, and impaired glycemic control. J Biol Chem. 2004; 279:41114–41123. [PubMed: 15272020]
27. Kang DH, Johnson RJ. Vascular endothelial growth factor: a new player in the pathogenesis of renal fibrosis. Curr Opin Nephrol Hypertens. 2003; 12:43–49. [PubMed: 12496665]

28. Kennedy B, Elayan H, Ziegler MG. Glucocorticoid hypertension and nonadrenal phenylethanolamine N-methyltransferase. Hypertension. 1993; 21:415–419. [PubMed: 8458643]
29. Lang CH, Frost RA. Endotoxin disrupts the leucine-signaling pathway involving phosphorylation of mTOR, 4E-BP1, and S6K1 in skeletal muscle. J Cell Physiol. 2005; 203:144–155. [PubMed: 15389631]
30. Locsey L, Asztalos L, Kincses Z, Gyorfi F, Berczi C. Dyslipidaemia and hyperlipidaemia following renal transplantation. Int Urol Nephrol. 1996; 28:419–430. [PubMed: 8899484]
31. Lodwick D, Kaiser MA, Harris J, Cumin F, Vincent M, Samani NJ. Analysis of the role of angiotensinogen in spontaneous hypertension. Hypertension. 1995; 25:1245–1251. [PubMed: 7768569]
32. Lu NZ, Cidlowski JA. Translational regulatory mechanisms generate N-terminal glucocorticoid receptor isoforms with unique transcriptional target genes. Mol Cell. 2005; 18:331–342. [PubMed: 15866175]
33. Mankoo BS, Collins NS, Ashby P, Grigorieva E, Pevny LH, Candia A, Wright CV, Rigby PW, Pachnis V. Mox2 is a component of the genetic hierarchy controlling limb muscle development. Nature. 1999; 400:69–73. [PubMed: 10403250]
34. McKay LI, DuBois DC, Sun YN, Almon RR, Jusko WJ. Corticosteroid effects in skeletal muscle: gene induction/receptor autoregulation. Muscle Nerve. 1997; 20:1318–1320. [PubMed: 9324091]
35. Ramakrishnan R, DuBois DC, Almon RR, Pyszczynski NA, Jusko WJ. Fifth-generation model for corticosteroid pharmacodynamics: application to steady-state receptor down-regulation and enzyme induction patterns during seven-day continuous infusion of methylprednisolone in rats. J Pharmacokinet Pharmacodynam. 2002; 29:1–24.
36. Ramakrishnan R, DuBois DC, Almon RR, Pyszczynski NA, Jusko WJ. Pharmacodynamics and pharmacogenomics of methylprednisolone during 7-day infusions in rats. J Pharmacol Exp Ther. 2002; 300:245–256. [PubMed: 11752123]
37. Reynolds RM, Walker BR. Human insulin resistance: the role of glucocorticoids. Diabetes Obes Metab. 2003; 5:5–12. [PubMed: 12542720]
38. Seo J, Hoffman E. Probe set algorithims: is there a rational best bet? BMC Bioinformatics. 2006; 7:395. [PubMed: 16942624]
39. Staels B, Dallongeville J, Auwerx J, Schoonjans K, Leitersdorf E, Fruchart JC. Mechanism of action of fibrates on lipid and lipoprotein metabolism. Circulation. 1998; 98:2088–2093. [PubMed: 9808609]
40. Sun YN, DuBois DC, Almon RR, Jusko WJ. Fourth-generation model for corticosteroid pharmacodynamics: a model for methylprednisolone effects on receptor/gene-mediated glucocorticoid receptor down-regulation and tyrosine aminotransferase induction in rat liver. J Pharmacokinet Biopharm. 1998; 26:289–317. [PubMed: 10098101]
41. Sun YN, DuBois DC, Almon RR, Pyszczynski NA, Jusko WJ. Dose-dependence and repeated-dose studies for receptor/gene-mediated pharmacodynamics of methylprednisolone on glucocorticoid receptor down-regulation and tyrosine aminotransferase induction in rat liver. J Pharmacokinet Biopharm. 1998; 26:619–648. [PubMed: 10485078]
42. Sun YN, McKay LI, DuBois DC, Jusko WJ, Almon RR. Pharmacokinetic/pharmacodynamic models for corticosteroid receptor down-regulation and glutamine synthetase induction in rat skeletal muscle by a receptor/gene-mediated mechanism. J Pharmacol Exp Ther. 1999; 288:720–728. [PubMed: 9918581]
43. Thissen JP. Towards an understanding of molecular mechanisms of muscle atrophy. [comment]. Curr Opin Clin Nutr Metab Care. 2005; 8:245–247. discussion 271–245. [PubMed: 15809525]
44. Tisdale MJ. Biochemical mechanisms of cellular catabolism. Curr Opin Clin Nutr Metab Care. 2002; 5:401–405. [PubMed: 12107376]
45. Wald JA, Farr RS. Abnormal liver-function tests associated with long-term systemic corticosteroid use in subjects with asthma. J Allergy Clin Immunol. 1991; 88:277–278. [PubMed: 1880328]
46. Wu Z, Irizzary RA. Preprocessing of oligonucleotide array data. Nat Biotechnol. 2004; 22:656–658. [PubMed: 15175677]

47. Wyzykowski JC, Winata TI, Mitin N, Taparowsky EJ, Konieczny SF. Identification of novel MyoD gene targets in proliferating myogenic stem cells. Mol Cell Biol. 2002; 22:6199–6208. [PubMed: 12167713]

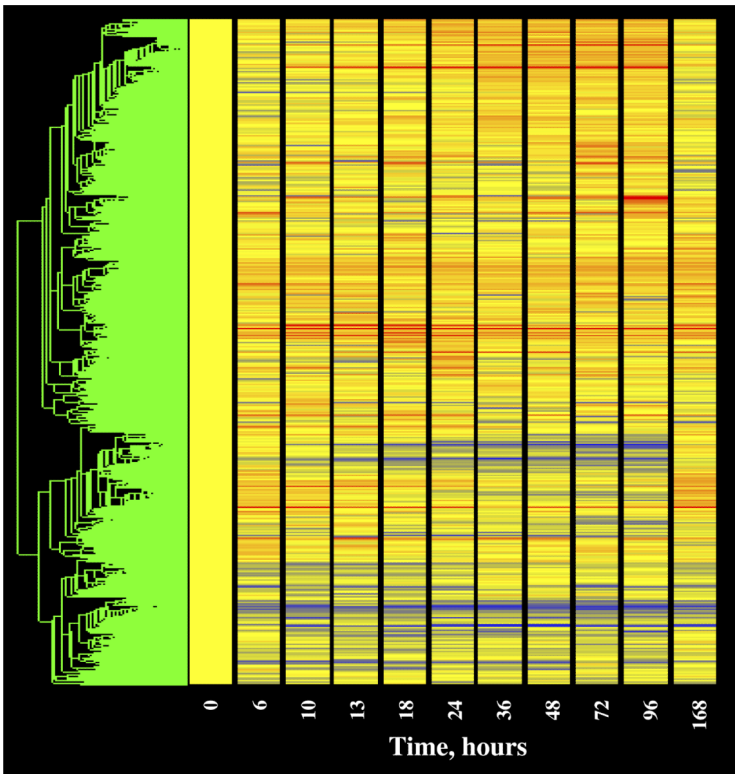

Fig. 1.

Gene tree representation of all probe sets (15,967) on individual Affymetrix R230A gene chips hybridized to total RNA prepared from muscles taken from animals treated chronically with methylprednisolone (MPL; 0.3 mg•kg^{-1}•h^{-1}) for periods ranging from 6 to 168 h. the values for each individual probe set at each time point were normalized to the mean value of that probe set for vehicle-treated controls. The *x*-axis represents the 11 time points, including vehicle-treated controls (nominal *time 0*). The *y*-axis presents the list of probe sets grouped by similarity using Pearson correlation. Yellow indicates no change from controls, red indicates probe sets with enhanced expression relative to controls, and blue indicates suppressed expression relative to controls.

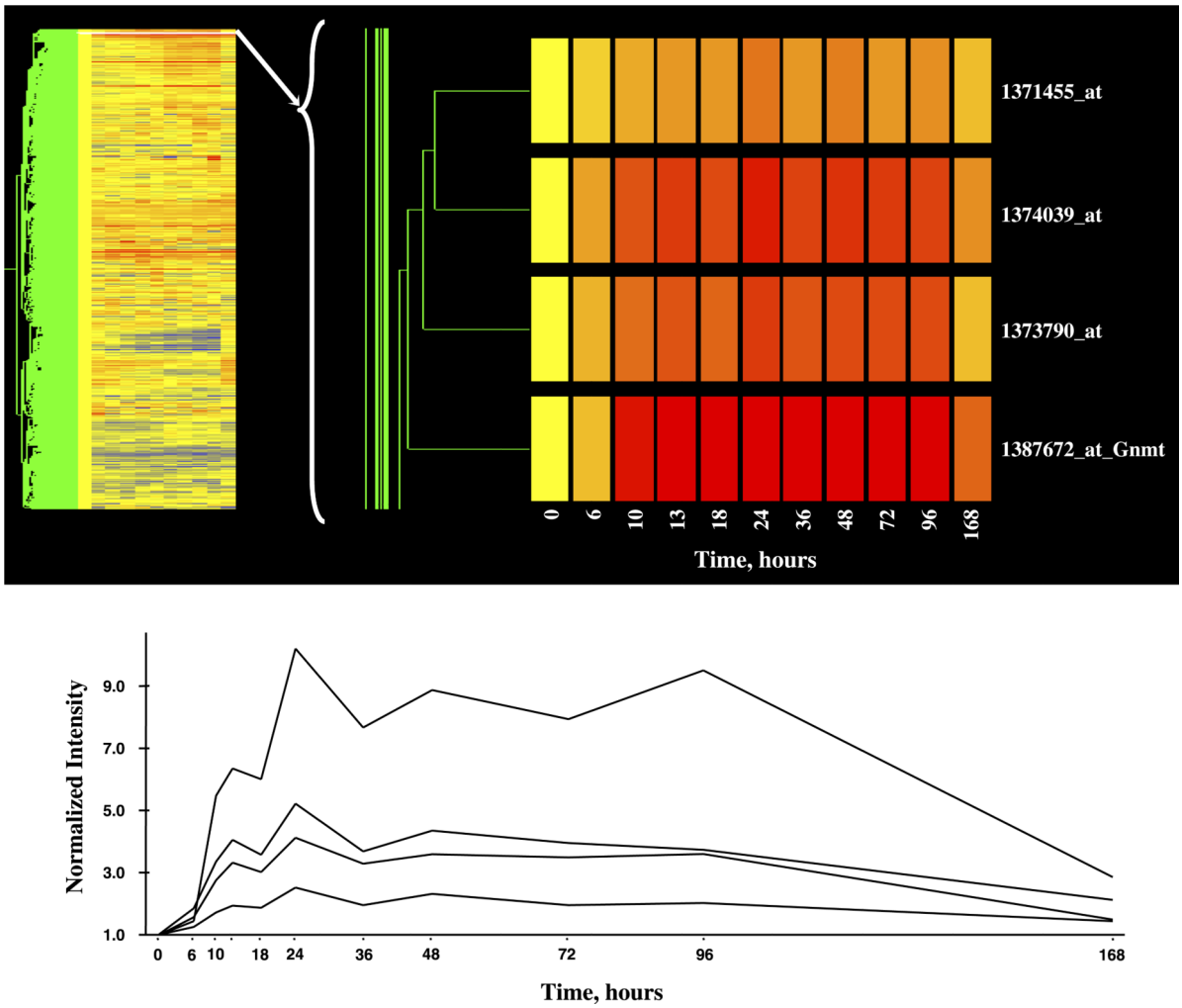

Fig. 2.

Top: a magnification of 4 probe sets selected from Fig. 1 that show apparent enhanced regulation by MPL. The linear plots for these probe sets are presented at *bottom*.

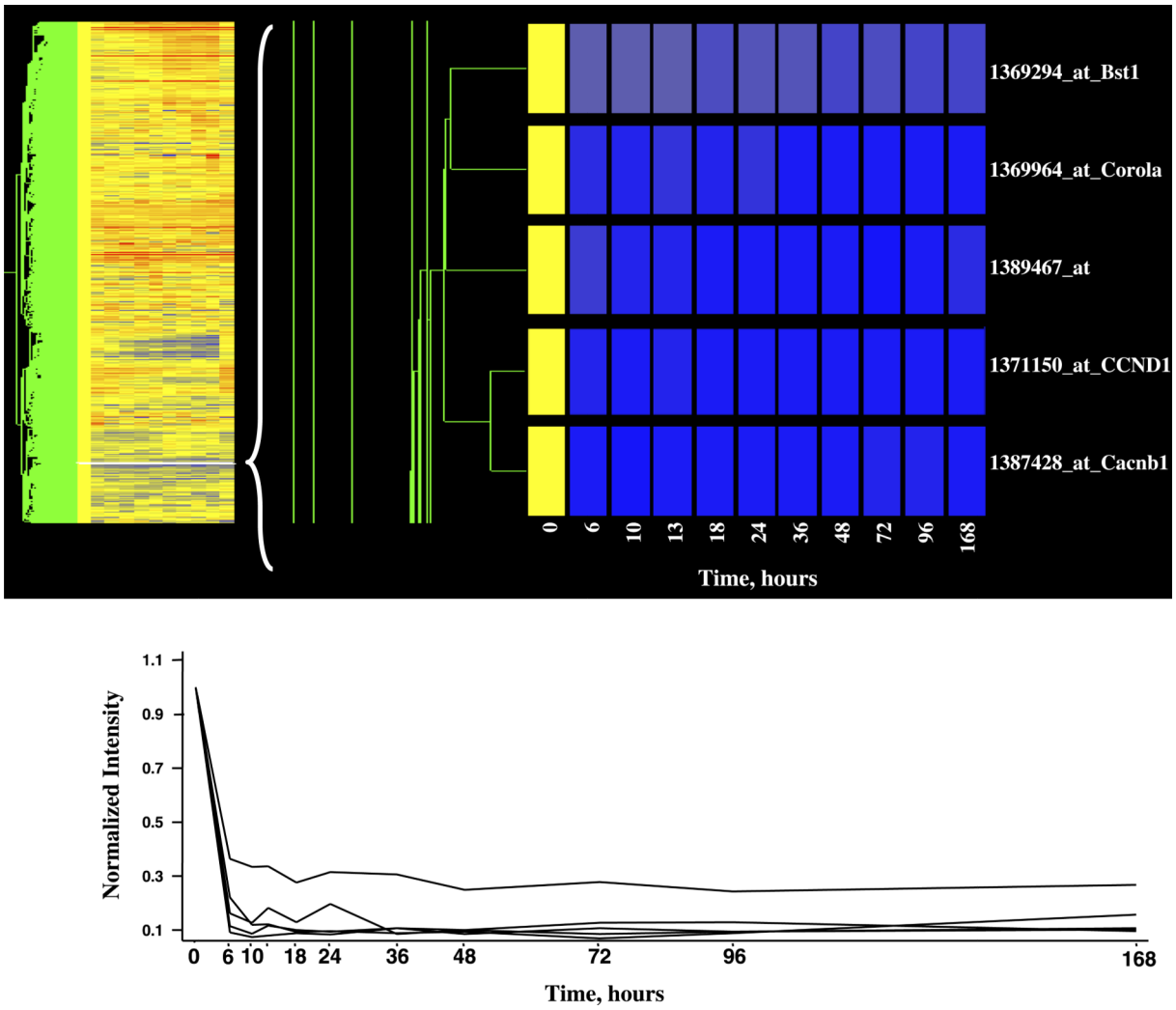

Fig. 3.

Top: a magnification of 5 probe sets selected from Fig. 1 that show apparent downregulation by MPL. The linear plots of all 5 probe sets are presented at *bottom*.

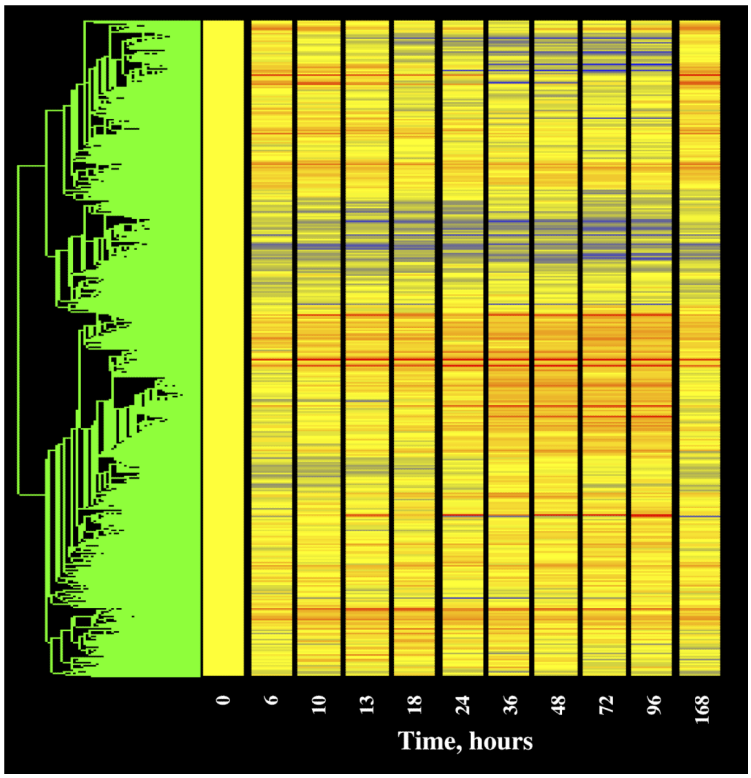

Fig. 4.

Gene tree representation of the 9,816 probe sets remaining after removing probe sets (6,151) that did not give a call of present using MAS5.0 software in at least 3 of 44 chips in the data set.

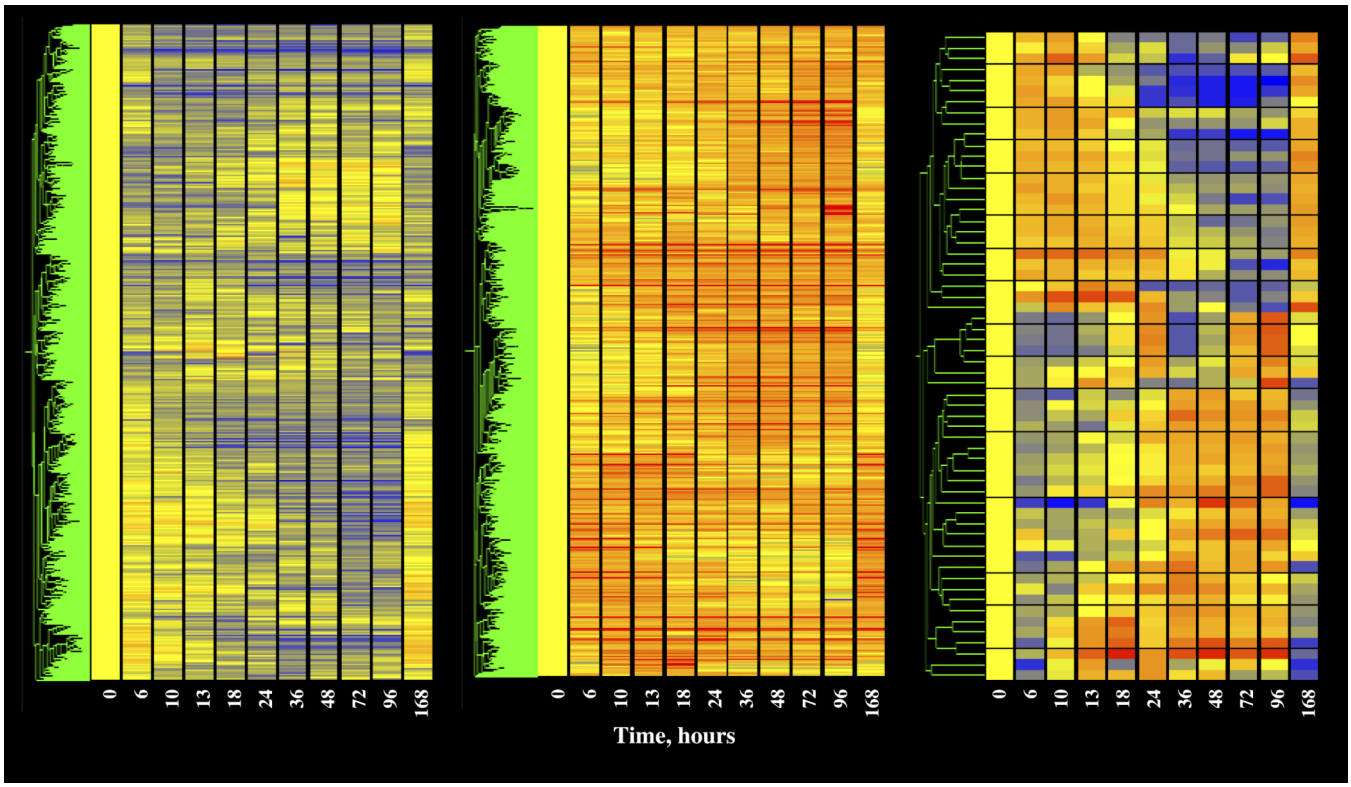

Fig. 5.

Gene trees of probe sets remaining after filtering for MPL regulation. *Left*: probe sets with potential downregulation (1,466). *Middle*: those with potential upregulation (1,412). *Right*: probe sets that met both criteria (60).

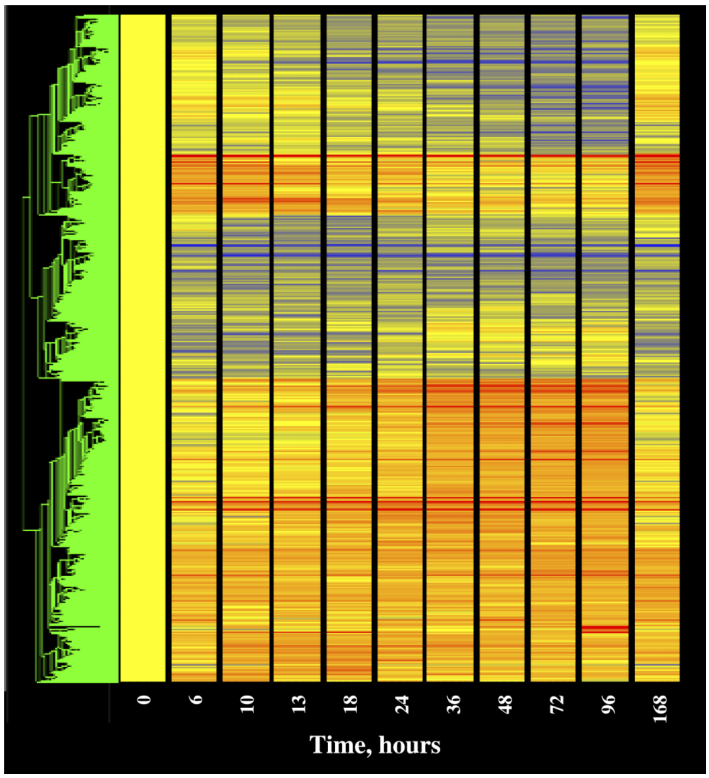

Fig. 6.

Gene tree representation of probe sets remaining (2,316) after filtering the probe sets in Fig. 5 for high coefficients of variation.

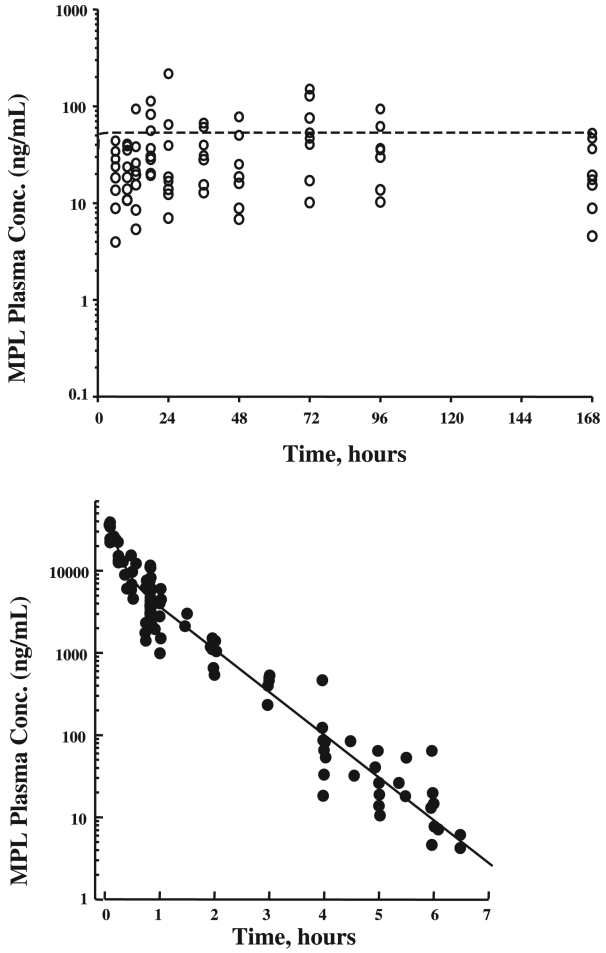

Fig. 7.

MPL concentrations in rat plasma following chronic (*top*) and acute (*bottom*) administration of drug. MPL concentrations were determined by normal-phase HPLC analysis of plasma samples obtained from individual animals.

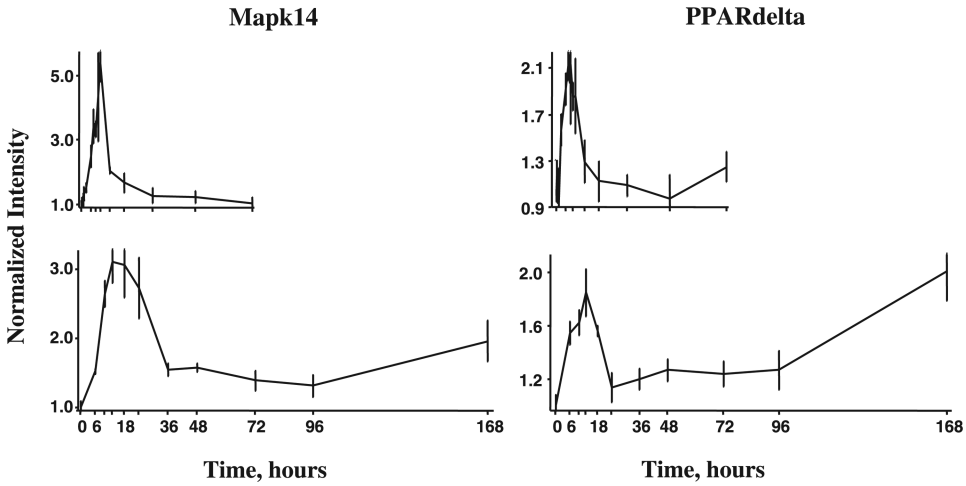

Fig 8.

Response profiles of 2 genes showing enhanced expression and tolerance with chronic dosing. Acute-dosing profiles are shown at *top*, and chronic-dosing profiles are shown at *bottom*. Mitogen-activated protein kinase-14 (MAPK14) expressions are shown at *left* and peroxisome proliferator-activated receptor-δ (PPARδ) at *right*.

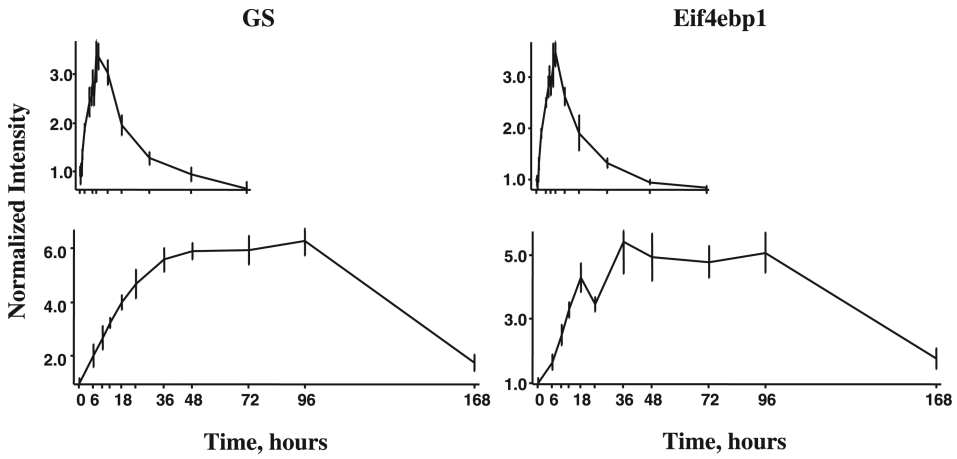

Fig. 9.

Response profiles of 2 genes showing enhanced expression but the absence of tolerance with chronic dosing. Acute-dosing profiles are shown at *top*, and chronic-dosing profiles are shown at *bottom*. Glutamine synthetase (GS) expressions are shown at *left* and eukaryotic translation initiation factor-4e binding protein-1 (Eif4ebp1) at *right*.

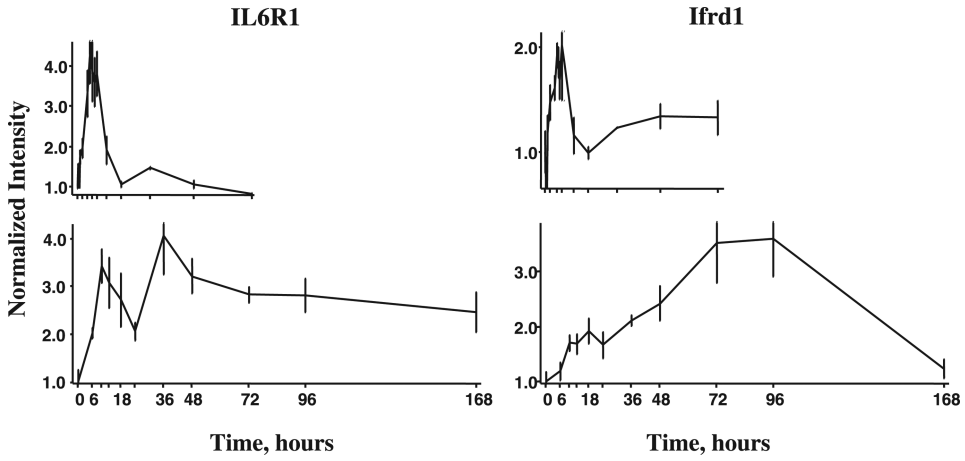

Fig. 10.

Response profiles of 2 genes showing both primary and secondary enhanced expression. Acute-dosing profiles are shown at *top*, and chronic-dosing profiles are shown at *bottom*. Interleukin-6 receptor (IL6R1) expressions are shown at *left* and interferon-related developmental regulator-1 (Ifrd1) at *right*.

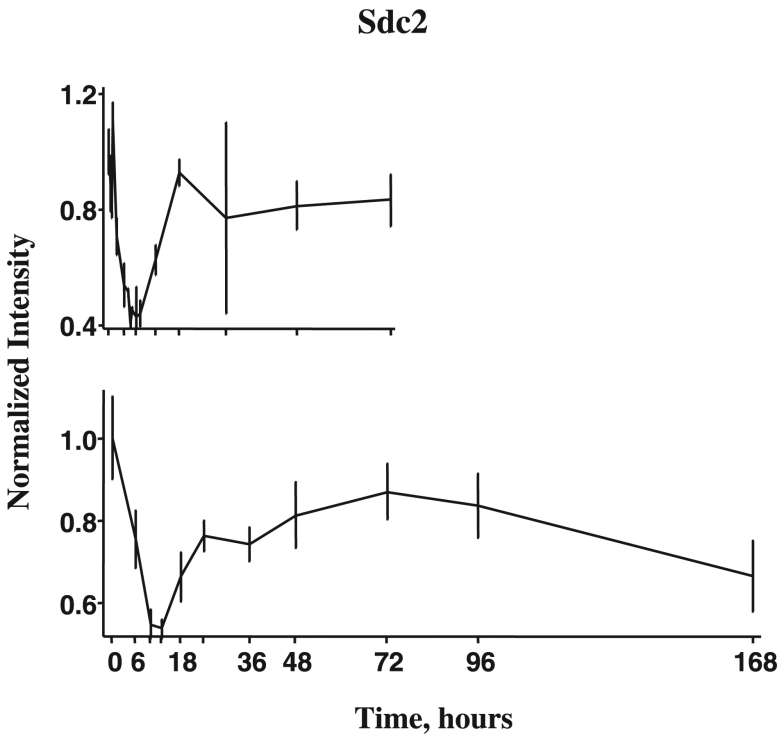

Fig. 11.

Response profiles of Syndecan 2 core protein (Sdc2), which shows decreased expression following MPL administration and only partial tolerance with chronic dosing. Acute-dosing profiles are shown at *top* and chronic-dosing profiles at *bottom*.

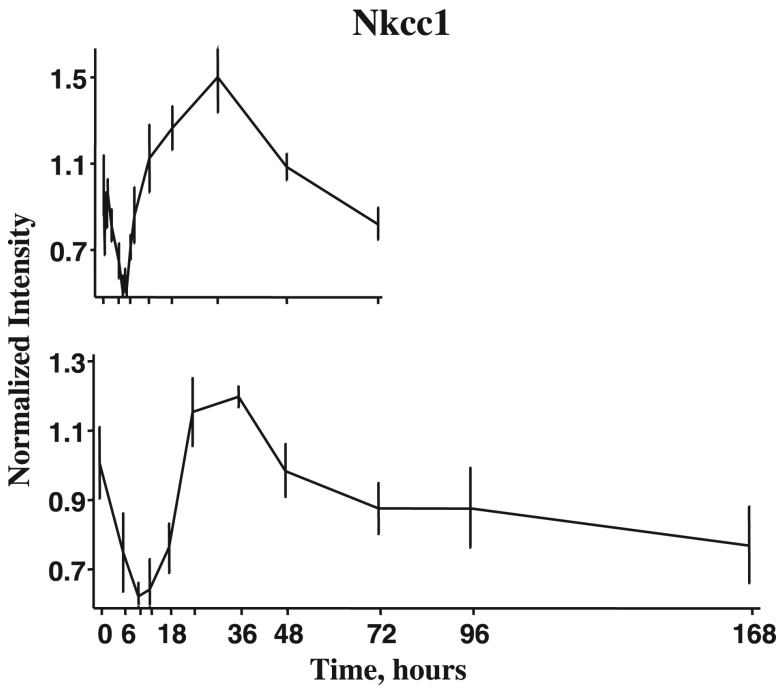

Fig. 12.

Response profiles of Na-K-Cl cotransporter (Nkcc1), which shows decreased expression following MPL administration and tolerance with chronic dosing. Acute-dosing profiles are shown at *top* and chronic-dosing profiles at *bottom*.

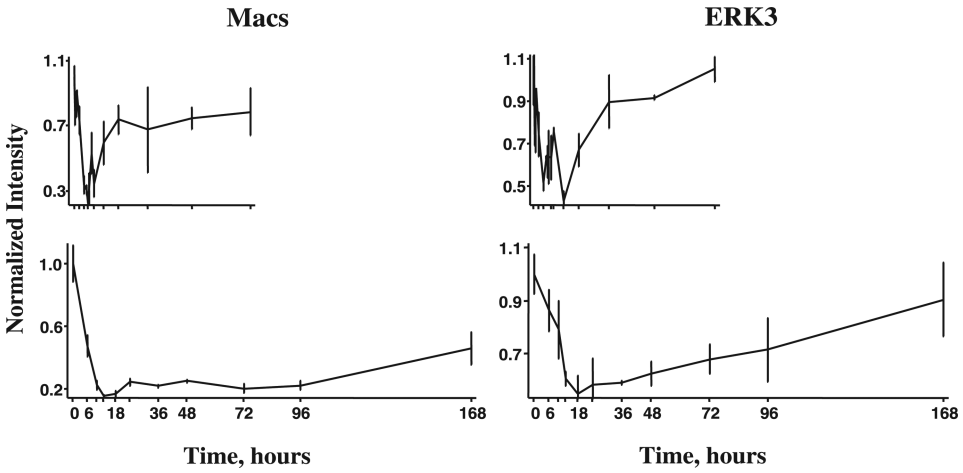

Fig. 13.

Response profiles of 2 genes showing decreased expression but absence of tolerance with chronic dosing. Acute-dosing profiles are shown at *top*, and chronic-dosing profiles are shown at *bottom*. Myristoylated alanine-rich C-kinase substrate (Macs) expression is shown at *left* and extracellular signal-related kinase-3 (ERK3) at *right*.

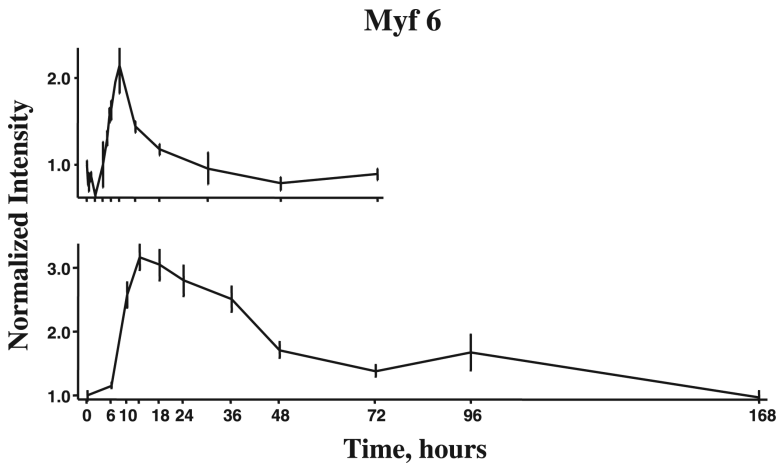

Fig. 14.

Response profiles of myogenic factor-6 (Myf6), which shows complex regulation of expression following acute (*top*) and chronic (*bottom*) MPL dosing. In the acute profile, there is an initial downregulation followed by a period of enhanced regulation.

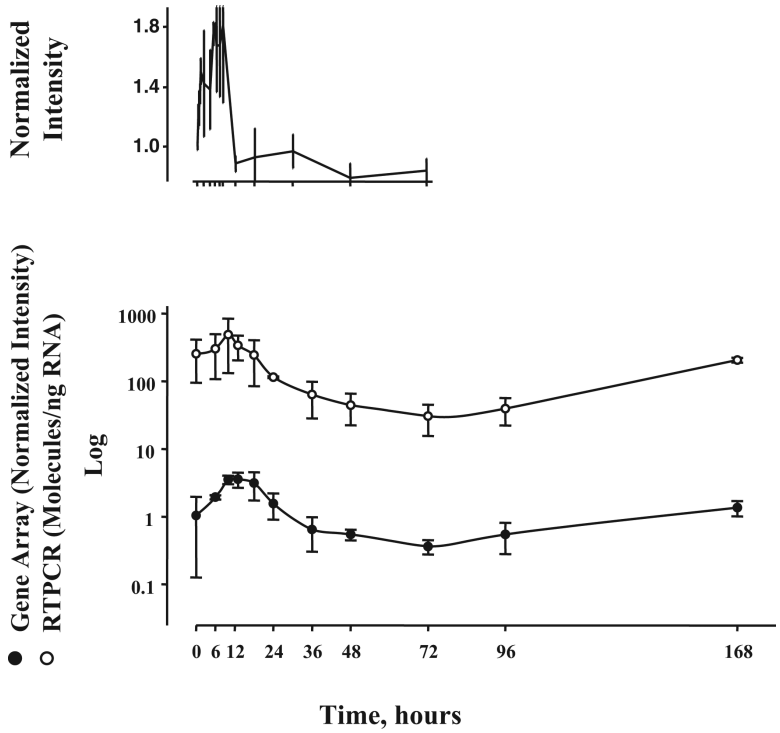

Fig. 15.

Response profiles of myostatin following acute dosing as determined from gene arrays (*top*) and following chronic dosing (*bottom*) as determined by both gene arrays (●) and by kinetic-based quantitative RT-PCR (○).

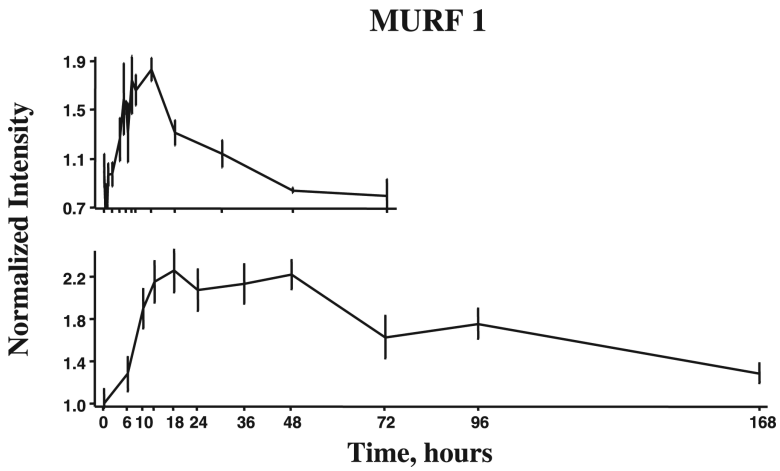

Fig. 16.

Response profiles of ring finger protein-28 (MURF1) following acute (*top*) and chronic (*bottom*) dosing.

Table 1

Methylprednisolone-regulated probe sets related to transcription-translation

Identification	Symbol	230A Probe Set No.	230A Accession No.	U34A Probe Set/Accession No.	Response	
					Acute	Chronic
V-ets erythroblastosis virus E26 oncogene homolog 1	Etsl	1368851_at	NM_012555	AI175900	down	down
Endoplasmic reticulum protein ERp29	Erp29	1387031_at	U36482	U36482	down	down
bZip transcription factor	Maf	1387165_at	NM_019318	AA893082	down	down
Gax protein; growth-arrest-specific protein	Meox2	1368422_at	NM_017149	Z17223	down	down
Myogenin	Myog, Myf4	1368310_at	NM_017115	M24393	down	down
Myogenic regulatory factor	MyoD	1398655_at	AA955902	M84174	down	down
NF1-B	Nfib	1371202, 1388167	AB012232, BE099050	AB012230	down	down
RAB3A, member RAS oncogene family	Rab3a	1369816_at	NM_013018	X06889	down	down
Splicing factor, arginine/serine-rich 10	Sfrsl0	1370188_at	AW252670	AA851749	down	down
MyoD family inhibitor domain containing	Mdfic	1374752_at	AI408734	AI639149	down	down
General transcription factor II I repeat domain containing 1	Gtf2ird1	1379550_a_at	BF290483	AA800912	down	down
Zinc finger and BTB domain containing 38	Zbtb38	1378009_at	BF282481	AA800768	down	down
Stem cell factor KL-1	stf	1388856_at	BG374178	AF071204	down	down
Sestrin 3	SESN3	1374350_at	BM382988	AA874873	down	down
Heterogeneous nuclear ribonucleoprotein A1	helix-destabilizing protein	1375612_at	AA965147	AA799893	up/down	down
Rev-ErbA-alpha protein; thyroid/steroid hormone receptor superfamily	Nrldl	1370816_at	M25804	M25804 (2)	down/up/	down
Cited2	Cited2	1367602, 1367601	AI013390, NM_053698	AA900476, AI014091	down	down/up
Thyroid hormone responsive SPOT14 homolog	Thrsp	1370150, 1387852	NM_012703 (2)	K01934	down/up	down/up
Myeloid differentiation primary response gene 116	Myd116	1370174_at	BI284349	AF020618	up	down/up
rhoB	Arhb	1369958_at	NM_022542	AA900505	up	up
ADP-ribosylation-like 4	Arl4	1367960_at	NM_019186	X77235	up	up
Aryl hydrocarbon receptor nuclear translocator 1	Arntl	1369244_at	NM_012780, AB012600	U08986, U61184	up	up
CCAAT/enhancer binding protein, delta	Cebpd	1387343_at	NM_013154	AI045030, M65149	up	up
Eukaryotic translation initiation factor 4E binding protein 1	Eif4ebp1	1386888_at	NM_053857	U05014, U05014	up	up
jun B proto-oncogene	Jun	1389528, 1369788, 1387788	BI288619	AI175959, AA945867	down	up
Kruppel-like factor 9	Klf9	1370209_at	BE101336	D12769 (2)	up	up

Identification	Symbol	230A Probe Set No.	230A Accession No.	U34A Probe Set/Accession No.	Response	
					Acute	Chronic
Immediate early gene transcription factor	Nr4a1	1386935_at	NM_024388	U17254 (2)	up	up
Nuclear protein 1 (protein p8)	Nuprl	1367847_at	NM_053611	AF014503	up	up
Apoptosis antagonizing transcription factor	Pawr	1368702_at	U05989	U05989	up	up
Zinc finger protein 36	ZFP36, TIS11	1387870_at	AB025017	X63369	up	up
Zinc finger protein, jumonji domain containing 1A	TF	1370975_at	AI172079	X59993	up	up
Peroxisome proliferative-activated receptor, delta	PPAR delta	1374914_at	AI230294	U40064, AI230294	up	up
Peroxisome proliferative-activated receptor, alpha	PPAR alpha	1383188_at	BM390716	AA866383	up	up
ERBB receptor Feedback inhibitor 1	Errfil	1373093_at	AI169756	AI169756	up	up
Poly(rC) binding protein 4	Mdfic	1371915_at	AW523679	AA891314	up	up
Fos-like antigen 2	Gtf2ird1	1373035_at	AI031032	AA875032	up	up
DNA binding protein (GATA-GT1)	Zbtb38	1374335_at	AA800786	AA800786	up	up
V-maf musculoaponeurotic fibrosarcoma oncogene family, protein K	stf	1372211_at	BI284461	AA799744	up	up
Basic transcription element binding protein 1	SESN3	1371864_at	AW524563	D12769 (2)	up	up
Ring finger protein 135	ubiquitin ligase activity	1377759_at	BG666928	AA800808	up	up
SH3 domain containing adapter protein isoform SETA-1x23	Sh3kbpl	1370419, 1387957	AF230520, AF255888	AA875172, AA875172	down	up
Ras-related protein	RablO	1368847_at	NM_017359	AI230406	down	up
Inhibitor of DNA binding	Idl	1387028_a_at	M86708	L23148	down/up	up
Myc family DNA binding protein, leucine zipper	Max	1387646_a_at	NM_022210	D14447	down/up	up
Myogenic factor 6 (herculin)	Myf6	1387181_at	NM_013172	M27151	down	down/up
DNA binding; Myc family; leucine zipper	Max	1372090_at	AI231566	D14447	down/up/down	up
Topoisomerase (DNA) II alpha	Top2a	1388650_at	BM385445	AA899854	down	up/down

Probe sets regulated by methylprednisolone in rat muscle following both acute and chronic drug administration, categorized as relating to either transcription or translation (transcription-translation). Affymetrix 230A arrays use a probe set no. distinct from GenBank accession nos., whereas U34A chips use a common probe set/GenBank accession no. for identification.

Table 2

Methylprednisolone-regulated probe sets related to cell signaling

Identification	Symbol	230A Probe Set No.	230A Accession No.	U34A Probe Set/Accession No.	Response	
					Acute	Chronic
Cholinergic receptor, nicotinic, alpha	Chrna1	1369843_at	NM_024485	X74832	down	down
2′,3′-Cyclic nucleotide-3′-phosphodiesterase	Cnp	1370693, 1387897	M18630, L16532	L16532	down	down
Ephrin A1	Efna1	1398273_at	NM_053599	AA892417, D38056	down	down
Insulin-like growth factor binding protein 5	Igfbp5	1370960, 1387348	BE104060, BE113270	AI029920, M62781	down	down
FLK1 kinase insert domain receptor (VEGF receptor 2)	Kdr	1367948_a_at	U93307	U93306	down	down
Myristoylated alanine-rich C-kinase substrate	Macs, MARCKS	1373432, 1375523, 1370948, 1370949	BE111604, BE108178, M59859(2)	AA859896, AA925762, AA899253, AA955167	down	down
Mitogen-activated protein kinase kinase kinase 1	Map3k1, MEKK1	1368871_at, 1378423_at	NM_053887, AI102620	AI102620	down	down
Extracellular signal-related kinase 3	Mapk6	1368273_at	NM_031622	M64301, M64301	down	down
cAMP phosphodiesterase	Pde4b	1369044_ a_at	AF202733	AA799729, M25350	down	down
Signal transducing adaptor molecule (SH3 domain and ITAM motif)2	Stam2	1390669_at	AI639410	AI639410	down	down
Integrin beta 1 binding protein 3	Itgb1bp3	1378423_at	AI639060	AI639060	down	down
Tyrosine-protein phosphatase, nonreceptor type 3	PTP-H1	1389362_at	AI317821	AA799812	down	down
Phospholipase A2, group IVA (cytosolic, calcium-dependent	Pla2 g4a	1387566_at	NM_133551	U38376	down	down
Kelch repeat and BTB (POZ) domain containing 3	Kbtbd3	1385972_at	AA800770	AA800770	down	down
Guanylate binding protein 2, interferon-inducible	Gbp2	1368332_at	NM_133624	M80367	up/down	down
Activin type IIB receptor	Acvr2b	1388179_at	AI548799	L10640	down	down/up
Insulin-induced growth response protein	Insig1	1367894_at	NM_022392	L13619	down/up	down/up
Adrenomedullin	Adm	1387219_at	NM_012715	D15069	up	up
SH3 domain binding protein	CR16	1370648, 1370596	U25281, U31159	U25281, U31159	up	up
Homer3	Homer3	1370212_at	AW253366	AB020879	up	up
Insulin-like growth factor binding protein 3	Igfbp3	1386881 _at	NM_012588	M31837, AI009405	up	up
130 kDa-Ins(1,4,5)P3 binding protein, phospholipase C-like 1	Plcl1	1368700 _at	NM_053456	D45920, AI072447	up	up
Mitogen-activated protein kinase 14	Mapk14, p38alpha	1367697_at	NM_031020	AA924542, U73142, U73142, AI171630, U91847, AI137862	up	up
3-Phosphoinositide-dependent protein kinase-1	Pdpk1	1370052_at	NM_031081	Y15748	up	up

Identification	Symbol	230A Probe Set No.	230A Accession No.	U34A Probe Set/Accession No.	Response	
					Acute	Chronic
Serine threonine kinase pim3	Pim3	1367725 _at	NM_022602	AF086624	up	up
Preoptic regulatory factor-1, deiodinase, iodothyronine, type II	Porf1, Dio2	1369885 _at	NM_022688	X53231	up	up
Pleckstrin homology, Sec7 and coiled-coil domains	Pscd1	1369517 _at	NM_053910	U83895	up	up
RhoGEF	EST	1393224_at	AW529774	AI638994	up	up
Cyclic ADP-ribose hydrolase	Cd38	1368975 _at	NM_013127	D29646	up	up
LIM zinc-finger protein, cysteine and glycine-rich protein 2	SmLIM, Csrp2	1370282_at	U44948	U44948	up	up
FK506 binding protein 3	Fkbp3	1388882 _at	AA891798	AI103874	down	up
Protein kinase inhibitor, alpha	Pkia	1387398 _at	AA996685	L02615	down	up
Protein tyrosine phosphatase SH-PTP2	SH-PTP2	1388379 _at	AI172465	U57499	down	up
Stem cell factor KL-1	Kitl	1370770_s_at	AF071205	AF071204	up/down	up
Diphtheria toxin receptor	Dtr, HB-EGF	1368983_at	NM_012945	L05489	down	up/down
Mitogen-activated protein kinase kinase 6	Map2k6	1387809_at	NM_053703	AI176689	down	up/down
Serum/glucocorticoid regulated kinase	Sgk	1367802_at	NM_019232	L01624	up/down	up/down

Probe sets regulated by methylprednisolone in rat muscle following both acute and chronic drug administration, categorized as relating to cell signaling. Affymetrix 230A arrays use a probe set no. distinct from GenBank accession nos., whereas U34A chips use a common probe set/GenBank accession no. for identification.

Table 3

Methylprednisolone-regulated probe sets localized to plasma membranes

Identification	Symbol	230A Probe Set No.	230A Accession No.	U34A Probe Set/Accession No.	Response	
					Acute	Chronic
CD36-related class B scavenger receptor	SRB1R, Scarbl	1367855, 1386956	AF071495, NM_031541	D89655, AF071495	down	down
Embigin	Emb	1368541_at	NM_053719	AJ009698	down	down
ATP-sensitive potasium channel	kir6.1	1368911_at	AB043636	D42145	down	down
Epithelial membrane protein-1	EMP-1	1371527_at	BI275741	Z54212	down	down
Alpha-N-acetyl-neuraminide-alpha-2,8-sialyltransferase 4	St8 sia4	1376624_at	BF288208	AA893663	down	down
Annexin A5	Anxa5	1386862_at	NM_013132	D42137	down	down
Ferroportin 1, solute carrier family 39	Slc40a1, FPN1	1390412_at	AI229664	U76714 (2)	down	down
Syndecan 2, core protein; sulphate proteoglycan	Sdc2	1370167_at	BG668421	M81687	down	down
Tuba1	Tuba1	1367579_a_at	BI285434	AA892333	up/down	down
Cd24	Cd24	1369953_a_at	BI285141	AI171462, U49062 (2)	down	down/up
Na-K-Cl cotransporter (Nkccl)	Slc12a2	1367853_at	NM_031798		down/up	down/up
Ankyrin isoform	Ank3	1370638_at	AF069525	AA963682	up	up
GPI-anchored ceruloplasmin	Cp	1368419_at	AF202115	AA817854, L33869	up	up
Potassium inwardly rectifying channel J12	Kcnj12	1369795_at	NM_053981	X78461	up	up
Sodium-coupled nucleoside transporter	Slc28a2	1368227_at	NM_031664	U66723	up	up
Slc3a2	Slc3a2	1398771_at	NM_019283	AB015433	up	up
Osteomodulin, osteoadherin	Omd	1387197_at	NM_031817	AF104362	up	up
Syndecan 4	Sdc4	1367721_at	NM_012649	S61868, S61868	up	up
Cysteine-rich secretory protein LCCL domain containing 2	Lgl1, Crispld2	1387922_at	AF109674	AA859581	up	up
Matrix Gla protein	Mgp	1367568_a_at	NM_012862	AI012030	up	up
Sodium channel, voltage-gated, type 1, alpha polypeptide	Scn1a	1369210_at	NM_030875	M22253	down/up	up
Transmembrane protein 142A	Tmem142a	1390031_at	BG378798	AA800218	down/up	up
ATPase Na^+/K^+ transporting beta 1 polypeptide	Atp1b1	1367814, 1386937	M14137, AI232036	AI112173, AI230614	down	up

Probe sets regulated by methylprednisolone in rat muscle following both acute and chronic drug administration, identified as localized to plasma membranes. Affymetrix 230A arrays use a probe set no. distinct from GenBank accession nos., whereas U34A chips use a common probe set/GenBank accession no. for identification.

Table 4

Immune-related methylprednisolone-regulated probe sets

Identification	Symbol	230A Probe Set No.	230A Accession No.	U34A Probe Set/ Accession No.	Response	
					Acute	Chronic
Latexin	Lxn	1367768_at	NM_031655	X76985	down	down
11/3R gene; MHC	RT1Aw2	1371171_at	M10094	X67504	down	down
Major histocompatibility complex class II	MHC class2	1370383_s_at	BI279526	X53054	down	down
Interleukin-33	IL33	1389581_at	BF390510	AA892986	down	down
Chemokine (C-X-C motif) ligand 2	Cxcl2	1368760_at	NM_053647	U45965	up	down
Vascular cell adhesion molecule-1	Vcam1	1368474_at	NM_012889	M84488	up/down	down
Platelet factor 4	Pf4	1371250_at	AI169104	AI169104	down	down
Interferon regulatory factor 7	Irf7	1383564_at	BF411036	AA799861	up/down/up	down/up/down
Arachidonate 5-lipoxygenase activating protein	Alox5ap	1369672_at	NM_017260	X52196	up	up
B-cell translocation gene 2, anti-proliferative	Btg2	1386994_at	NM_017259	M60921	up	up
Complement component 1, q subcomponent, beta	C1qb	1370215_at	AW434057	X71127	up	up
Cytokine-inducible SH2 containing protein	Cish	1388233_at	AF065161	AF065161	up	up
T-cell receptor signal transduction	Lnk	1367723_a_at	NM_031621	AA943555, U24652	up	up
Interferon gamma receptor	Ifngr	1369956_at	NM_053783	U68272	up	up
Interferon-related developmental regulator 1	Ifrd1	1367795_at	NM_019242	AI014163	up	up
IL-15	IL-15	1368375_a_at	AF015718	AF015719	up	up
Interleukin 6 receptor	Il6r	1386987_at	NM_017020	M58587	up	up
Lipocalin 2	Lcn2	1387011_at	NM_130741	AA946503	up	up

Probe sets regulated by methylprednisolone in rat muscle following both acute and chronic drug administration, categorized as immune related. Affymetrix 230A arrays use a probe set no. distinct from GenBank accession nos., whereas U34A chips use a common probe set/GenBank accession no. for identification.

Table 5

Vascular-related methylprednisolone-regulated probe sets

Identification	Symbol	230A Probe Set No.	230A Accession No.	U34A Probe Set/Accession No.	Response	
					Acute	Chronic
Endothelial cell-specific molecule 1	Esm1	1368078_at	NM_022604	AI233219	down	down
Neuropilin 1	Nrp1	1373577_at	BE116566	AF016296	down	down
Cysteine-rich protein 61	Cyr61, IGFBP10	1368290_at	NM_031327	AA800784	up	down
Placental growth factor	Pgf	1368918_at	NM_053595	L40030	up	up
Prostaglandin-endoperoxide synthase 1, CYCLOOXYGENASE1	Ptgs1, COX-1	1368259_at	NM_017043	U03388	up	up
Endothelin converting enzyme 1	Ece1	1367801_at	NM_053596	D29683	up	up
Multimerin 1	Mmm1	1392053_at	AI639113	AI639113	up	up
Angiotensin converting enzyme	Ace	1387791_at	AF201331	L36664, AA800722, U03734	up	up
Group-specific component (vitamin D binding protein)	Gc	1368288_at	NM_012564	M12450	up	up
Cysteine-rich secretory protein LCCL domain containing 2	Crispld2	1376457_at	AI175861	AA859581	up	up
Vascular endothelial growth factor	Vegf	1373807_at	AI175732	L20913	up	up
Phosphatidylserine-specific phospholipase A1	Pspla1	1370445_at	D88666	D88666	up	up
Albumin	Alb	1367556_s_at	NM_134326	AA866237	up	up
Pleiotrophin (Heparine binding factor)	Ptn	1369968_at	NM_017066	AI102795	up/down	up/down
Angiopoietin-2	ANGPT2	1374207_at	BI275292	AF030378	up	up/down
Periostin	Postn	1373911 _at	BM389026	AA894092	down/up/down	up/down

Probe sets regulated by methylprednisolone in rat muscle following both acute and chronic drug administration, categorized as vascular. Affymetrix 230A arrays use a probe set no. distinct from GenBank accession nos., whereas U34A chips use a common probe set/GenBank accession no. for identification.

Table 6

Methylprednisolone-regulated probe sets related to protein or amino acid metabolism

Identification	Symbol	230A Probe Set No.	230A Accession No.	U34A Probe Set/Accession No.	Response	
					Acute	Chronic
Neuraminidase 2	Neu2	1368127_at	NM_017130	AI171959	down	down
Heat shock 27 kDa protein 1	Hspb1	1367577_at	NM_031970	AI176658	down/up	down/up
Heat shock 70kD protein 1A	Hspa1a	1368247_at	NM_031971	AA818604	down/up	down/up
Heat shock protein 70 protein 2	hsp70	1388900_at	BG381414	AA875620	up	up
Heat shock protein 40-3, or DnaJ subfamily B, member 5	Hsc40-3	1372144_at	BM386741	AA891542	up	up
Glutamine synthetase	Glul	1367633, 1386870, 1367632	BI296610, BI275294, NM_017073	M91652 (2),AA852004	up	up
Ring finger protein 28; muscle ring finger protein 1	Rnf28, MURF1	1372639_at	AA800245	AA800245	up	up
Ubiquitin-conjugating enzyme E2G 2	Ube2 g2	1371814_at	BI282191	AA859722	up	up
Tac2-N membrane targeting (tandem) C2 domain containing	Mtac2d1	1383606_at	BI302544	AI639417	up	up
Contrapsin-like protease inhibitor	Spin2c	1368224_at	NM_031531	D00753	up	up
Fumarylacetoacetate hydrolase	Fah	1368092_at	NM_017181	M77694	up	up
Proteasome (prosome, macropain) activator subunit 4	Temo, Psme4	1368818, 1368817	AW531920, AI180458	AA893664	up	up

Probe sets regulated by methylprednisolone in rat muscle following both acute and chronic drug administration, categorized as relating to protein or amino acid metabolism. Affymetrix 230A arrays use a probe set no. distinct from GenBank accession nos., whereas U34A chips use a common probe set/GenBank accession no. for identification.

Table 7

Nuclear-encoded mitochondrial genes regulated by methylprednisolone

Identification	Symbol	230A Probe Set No.	230A Accession No.	U34A Probe Set/ Accession No.	Response	
					Acute	Chronic
Creatine kinase	Ckb	1367740_at	M14400	M57664	down	down
Diacylglycerol kinase zeta	Dgkz	1367745_at	NM_031143	D78588	down	down
L-arginine: glycine amidinotransferase	Gatm	1367627_at	NM_031031	U07971	down	down
Glycerol-3-phosophate dehydrogenase 2	Gpd2	1369666_at	BG378763	X78593	down	down
NADH:ubiquinone oxidoreductase MLRQ subunit	–	1389018_at	BF411239	AA686870	down	down
Microsomal glutathione-S-transferase 1	Mgst1	1367612_at	NM_134349	J03752	down	down
Cytochrome c, somatic	Cycs	1387773_at	NM_012839	K00750	down	up
Mitochondrial cytochrome P-450 (P450C27)	CYP27	1387914_at	M73231	Y07534, M38566	up	up
Uncoupling protein 3	Ucp3	1387681_at	U92069	AF030163, AF035943	up/down	up
Pantothenate kinase 2	Pank2	1374541_at	BM392117	AA891438	down	up

Probe sets regulated by methylprednisolone in rat muscle following both acute and chronic drug administration, identified as nuclear-encoded mitochondrial genes. Affymetrix 230A arrays use a probe set no. distinct from GenBank accession nos., whereas U34A chips use a common probe set/GenBank accession no. for identification.

Table 8

Other methylprednisolone-regulated probe sets

Identification	Symbol	230A Probe Set No.	230A Accession No.	U34A Probe Set/Accession No.	Response	
					Acute	Chronic
Isocitrate dehydrogenase 1, soluble	Idh1	1369954_at	NM_031510	AA892314	down	down
Fatty acid Coenzyme A ligase, long chain 3	Facl3	1368177_at	NM_057107	D30666	down	down
Microtubule-associated protein tau	Mapt	1387071, 1368138	BE107978, BI281170	AI227608	down	down
Myosin-IC	Myo1e	1370933_at	BI275813	AI175935	down	down
Dynein, cytoplasmic, light chain 1	Pin, Dnclc1	1369976, 1388384	NM_053319, AI407618	AI009806 (2)	down	down
Aldehyde dehydrogenase	Aldh1a2	1368003_at	NM_053896	U60063	down	down
Lumican	Lum	1367749_at	NM_031050	X84039	down	down
Procollagen, type XV	Col15a1	1388939_at	AA800298	AA800298	down	down
Alpha-tropomyosin 2	TPM2	1379936, 1390471	AA875132, BM38341	AA875132, M60666	down	down
EST	EST	1388880_at	BI278962	AI177256	down	down
EST	EST	1374767_at	AI105450	AA799396 (2)	down	down
UDP-glucose:ceramide glycosyltransferase	Ugcg	1387975_at	AF047707	AF047707 (2)	up	down
Chondroadherin	Chad	1368788_at	NM_019164	AF004953	up	down
Matrix protein; osteopontin; sialoprotein	Spp1	1367581_a_at	AB001382	M14656	up	down
Adenosine monophosphate deaminase 3	Ampd3	1368342_at	NM_031544	U90888	up	down
Kinesin, light chain	Klc1	1370886_a_at	AA944723	M75148	up	down
EST	EST	1394126_at	AA893693	AA893693	up	down
Glutathione peroxidase 3	Gpx3	1369926_at	NM_022525	D00680	down/up	down/up
Nucleotide binding protein-like	Nubpl	1376659_at	BF282469	AA892306	down/up	down/up
S-adenosylmethionine decarboxylase 1	Amd1	1367933_at	NM_031011	AI008131	up	up
Bcl-xalpha	Bcl2l	1370812_at	U72350	U72350, U34963	up	up
6-Phosphofructo-2-kinase/fructose-2,6-biphosphatase 4	PFKFB	1389396_at, 1369794_a_at	BE329273, D87247	M64797, D87240	up	up
Microsomal glutathione-*S*-transferase 2	Mgst2	1372599_at	BI290559	AA955983	up	up
Flavin containing monooxygenase 1	Fmo1	1387053_at	NM_012792	M84719	up	up
Sulfotransferase family 1A, phenol-preferring, member 1	Sult1a1	1370019_at	AF394783	L19998 (2)	up	up
Cytosolic cysteine dioxygenase 1	Cdo1	1367755_at	NM_052809	AA942685	up	up
Cyp4b1	Cyp4b1	1370399_at	M29853	M29853	up	up

Physiol Genomics. Author manuscript; available in PMC 2014 October 06.

Identification	Symbol	230A Probe Set No.	230A Accession No.	U34A Probe Set/Accession No.	Response	
					Acute	Chronic
Trichohyalin	Tchh	1386160_at	AI639401	AI639401	up	up
EST	EST	1388336_at	AI411514	AA799537	up	up
Actin alpha cardiac 1	Actc1	1370856_at	AA800705	AA866452, AI104567 (2)	down	up
DNA pol	Polb	1368341_at	M13961	J02776	down	up
Stearyl-CoA desaturase	Scd1	1370355_at	J02585	J02585	down	up/down
Hypoxia induced gene 1	Hig1	1370062_at	NM_080902	H31665	down/up/down	up

Probe sets regulated by methylprednisolone in rat muscle following both acute and chronic drug administration but uncategorized. Affymetrix 230A arrays use a probe set no. distinct from GenBank accession nos., whereas U34A chips use a common probe set/GenBank accession no. for identification. EST, expressed sequence tag.